Open access • Journal Article • DOI:10.1080/10408437308245837

The interaction of molecular beams with solid surfaces — Source link

G. A. Somorjai, S. B. Brumbach

Published on: 01 Aug 1973 - Critical Reviews in Solid State and Materials Sciences (Taylor & Francis Group)

Topics: Inelastic scattering, Elastic scattering and Inelastic neutron scattering

LBL-2212
CONF-730847--1

THE INTERACTION OF MOLECULAR BEAMS WITH SOLID SURFACES

G. A. Somorjai and S. B. Brumbach

Inorganic Materials Research Division, Lawrence Berkeley Laboratory
and Department of Chemistry; University of California,
Berkeley, California 94720

I. Introduction

In recent years, a great variety of experimental techniques has become available that permits study of the clean surface and the solid-gas interface on an atomic scale. The structure of surfaces and of adsorbed gases and the chemical composition of the topmost layer at the surface are being studied by low energy electron diffraction and electron spectroscopy (photoelectron spectroscopy, Auger electron spectroscopy, appearance potential spectroscopy, ion neutralization spectroscopy, etc.). Low energy electron beams (1-1000 eV) are particularly applicable to investigate the atomic properties of the surface because of their low penetration and large cross sections for excitation of both the electrons and phonons of the solid surface. Atomic and molecular beams are perhaps even more surface sensitive than low energy electrons. Emanating from a room temperature source their kinetic energy is about 0.02 eV, 2-4 orders of magnitude lower than that of low energy electrons. Since chemical bond energies are in the range of 0.5-10 eV, collision of incident atoms with atoms in the surface will not result in breaking of chemical bonds. Like electrons, atoms are scattered by the atomic potential, and their

penetration below the surface is negligible. If atomic beams are surface sensitive, then why not use them to the same extent as low energy electrons for surface studies? In present-day technology it is much easier to generate and control (collimate, scatter and detect) charged particles than a beam of neutral species. Atomic beam scattering studies at present require special techniques newly developed to measure the energy and spatial distribution of particles. Nevertheless, generation and detection of atomic beams has been developed in the past several years to the point where molecular beam-surface scattering experiments can be carried out in most laboratories with relative ease using commercially available apparatus.

Just as low energy electron diffraction and electron spectroscopy are very well suited to determine the structure and composition of solid surfaces, molecular beam scattering provides us with detailed information on the energy transfer during surface reactions. By measuring the velocity and angular distribution of the incident beam and the beam scattered from the surface, one can determine the partitioning of the energy evolved in the surface chemical reaction between the reactants and the surface and among the reaction products. Thus, like crossed molecular beam gas phase reaction studies, surface scattering studies reveal the elementary energy transfer steps in surface reactions. The dynamics of surface reactions on an atomic scale are at our disposal from molecular beam scattering studies of gas-surface interactions.

In this chapter, we shall describe the molecular beam-surface scattering experiments, the nature of scattering (elastic, inelastic) and the

experimental information that can be obtained from detection of the angular distribution and the kinetic energy of the scattered particles. We shall discuss the types of energy exchange that take place between a gas atom or molecule and the surface atoms and the theories that have been developed to explain some of these energy transfer processes. We shall then review the results of some molecular beam-surface scattering experiments and point out directions for future investigation. We shall discuss most of the pertinent topics only briefly but provide references for the reader interested in exploring this important and rapidly developing field of surface science in greater detail. Attention should be called to other recent reviews that are available in the literature.[1-4]

II. The Molecular Beam-Surface Scattering Experiment

A. Vacuum System

A typical molecular beam vacuum system has three basic components, a beam source, a scattering surface and a detector for scattered particles. These components may be in separate, differentially pumped chambers. The design of the vacuum system is dominated by two competing considerations. The first is the desire to keep the pressure in the scattering chamber low to maintain a scattering surface as clean as possible and to reduce the number of gas phase collisions. The second is that because of severe signal attenuation in the scattering process, it is desirable to have an incident beam as intense as possible so that acceptable signal levels can

be obtained. The separate pumping of the detector chamber can also greatly enhance the signal-to-noise ratio by removing background gases. A typical vacuum system is shown in block diagram form in Figure 1.

B. Sample Preparation and Treatment

It is necessary to have a scattering surface where the chemical composition, presence of adsorbed layers, atomic structure and roughness are well defined to make a meaningful interpretation of scattering results. Several methods have been used to produce and maintain clean surfaces for scattering. One can begin with a well defined single crystal surface and keep the scattering chamber pressure below about 10^{-9} torr.[5-7] This requires ultra high vacuum hardware and techniques. As a means of monitoring the composition of the surface, Auger electron spectroscopy can be used,[5] and Low Energy Electron Diffraction can monitor the surface structure.[5-8] One may carry out scattering studies from surfaces at sufficiently high sample temperatures that impurity gases do not adsorb because of their low sticking probability and short surface resident time. This technique was investigated by Yamamoto and Stickney[9] with scattering from tungsten surfaces. Still another method is that of in situ deposition of a metal film on a substrate at a rate faster than that at which it becomes contaminated. This procedure was developed by Smith and Saltsburg[10] and has since been used in a wide variety of experiments.[11-13] While the film surface can be oriented in a particular crystallographic direction, recent experiments by Sau and Merrill[8] indicate that there is significantly more disorder

on an epitaxially grown film than on a well-annealed low Miller index single crystal surface. This was determined by monitoring the angular distribution of scattered helium atomic beams which proved to be very sensitive to surface disorder.[14,15]

C. Beam Sources

1. Effusion Sources

The effusion oven is the classical means of obtaining a molecular beam. A gas at relatively low pressure (less than 1 torr) is allowed to effuse through a small orifice (such that the mean free path of the gas is large compared to the dimensions of the orifice). A collimated beam is formed by pumping the gas through one or more subsequent orifices. The effusing particles have a Maxwellian velocity distribution characteristic of the temperature of the oven and have a cosine spatial distribution. The problem with such sources is their low intensity – typically 10^{13} - 10^{15} particles $str^{-1}sec^{-1}$ – because of the limitation on the pressure in the effusion cell to maintain effusion conditions. Because of the cosine distribution, a large fraction of the effusing molecules are pumped away in the collimating process.

2. Nozzle Beams

When a gas at a pressure of about 100 torr or greater is expanded adiabatically into vacuum, the enthalpy of the high pressure gas is converted

into net translational motion. If such a gas flow is properly collimated, it is possible to generate a very intense molecular beam as discussed recently by Anderson, Andres and Fenn.[16] With such beam sources intensities of 10^{18} - 10^{19} particles $str^{-1}sec^{-1}$ have been reported.[17] Using seeded beams[18] very high kinetic energies, in excess of 10 eV, are available. In seeded beams the velocity distribution in the beam is very narrow, corresponding to temperatures as low as 4°K.[19] The rotational temperature for a diatomic molecule in the nozzle beam is also reduced although not as much as the translational temperature.[19] Many investigators have used nozzle sources to generate beams for surface studies, and it is a particularly useful technique when one is investigating scattering as a function of incident beam energy.[20] The nozzle beam sources require very large (generally a few thousand litre sec^{-1}) pumping speeds to handle the associated large gas flows.

3. Multi-channel Arrays

A compromise between the low intensity effusion sources and the high intensity nozzle beam with its large pumping speed requirement is the multi-channel array source.[21-24] This source consists of a small bundle of about 4000 capillary tubes, each a few microns in diameter and about a millimeter long. The array diameter is also on the order of a millimeter. The normal gas pressure behind such a source is on the order of a few torr. This source shows peaking of intensity along the center line of the beam considerably in excess of that for an effusion source.[21]

This can increase the beam intensity by an order of magnitude over the effusion source. The velocity distribution in a multi-channel array beam is nearly, though not quite, Maxwellian.[23]

D. Signal Detection

1. Ionization Detectors

The most common detector for scattered molecular beams uses electron impact ionization. This can be a nude ionization gauge which measures total gas density or a small mass spectrometer, generally a quadrupole device which measures the partial pressure of a desired component of the scattered gas. The ionization detectors usually measure the density of the scattered gas, not the flux. Thus, while the velocity of the incident particles is considered implicitly in measuring the flux, a density sensitive detector is sensitive to changes in the velocity of the incident molecules. This must be kept in mind when velocity analysis of scattered particles is attempted.

Generally it is best to place the detector as close to the scattering surface as practical. If, for example, the molecules are scattered with a cosine distribution, the signal intensity will decrease with the square of the surface-detector distance. Similarly, it is also desirable to keep the incident beam-surface distance short although this is not as important if the beam is well collimated. If the angular distribution of scattered particles is studied, it is customary to have the detector mounted on a rotatable

feedthrough, and the scattering surface is then also made rotatable.

It should be mentioned that with present-day electron impact ionization no more than one out of 10^3 or 10^4 atoms incident on the detector is ionized. This low detector efficiency limits the sensitivity of molecular beam-surface scattering experiments.

2. Electronic Signal Processing

The output from the ion gauge or mass spectrometer detector is generally a dc current which can be measured with a simple electrometer. However, in most realistic molecular beam experiments the dc signal level of interest will be very small and the signal-to-noise ratio rather poor (noise being due to ionization of background gas molecules), requiring a more complex approach to signal extraction. The most common technique used is that of ac phase-sensitive detection. Here the beam is modulated mechanically by a rotating slotted disc or a vibrating tuning fork between the source and the detector. A reference signal is also produced by simultaneously chopping a light beam. This ac technique allows a weak modulated signal to be detected in a relatively large background gas pressure.

E. Measurement of Average Velocities and Velocity Distributions

In addition to improving the signal-to-noise ratio in beam experiments, the phase-sensitive ac method can also give information about the time of flight of the molecules between their chopping point and the detector. This information is contained in the shift of phase angle at maximum signal

intensity compared to the phase of the chopper. For instance, if one were to chop the scattered beam, assuming it is Maxwellian, then one can obtain the average translational energy (temperature) of the beam from the length of flight path, chopping frequency, molecular weight and phase shift.[25-29] Furthermore, if one can measure both the phase shift and signal amplitude as a function of modulation frequency, then a complete velocity distribution can be obtained.[23] Similarly, if the beam is chopped before striking the crystal, the time dependence of the gas-solid collision can be investigated — in particular, surface residence times can be measured.[28,29] If one is investigating a reactive scattering event, the time dependence of the process can be measured via phase shifts to yield information about the kinetics of the reaction,and these results can be compared to model systems.[28-30] Phase shift measurements, in order to be meaningful, require careful measuring of the phase and amplitude of the detector signals with respect to stable reference signals, measurements which are not at all simple in most practical beam experiments.

If one is interested in measurements of the velocity of the scattered molecular beam, an alternative to the phase shift measurement is the so-called "time of flight" technique.[31-33] Briefly, in this method a narrow pulse of molecules is allowed to traverse a flight path and is detected by a multi-channel signal averaging instrument where the signal intensity as a function of time is measured and stored. After many cycles a complete intensity vs. time of flight curve is obtained. The disadvantages of this method are the weak signal,due to short "on time" periods for the beam,and

the need to know the effects of instrumentation alone on the resulting waveform. Data obtained in such an experiment are generally presented as average energy and the "energy spread" characteristic of the beam temperature. It should be mentioned that for velocity analysis the classical method of rotating slotted disc velocity selectors can also be used. This method, however, suffers from signal attenuation by relatively low throughputs for most velocity selectors since most of the molecules are lost in the selection process.

F. Measurement of Angular Distributions

A convenient means of obtaining and presenting data characterizing a molecular beam-surface scattering process is the scattered beam angular distribution. Two important features of the distribution are generally discussed; the angle of the intensity maximum of the scattered beam with respect to the angle of the incident beam and its peak width at half maximum. Most measurements are "in-plane," which means that the angular distribution is measured in the plane defined by the incident beam and the surface normal. If the angle at which the scattered beam has maximum intensity, θ_r (measured with respect to the surface normal), equals the angle of incidence of the incoming beam, θ_i (also measured with respect to the surface normal), the scattering is said to be specular. If θ_r is between θ_i and the surface normal, the scattering is called subspecular. If $\theta_r > \theta_i$, the scattering is supraspecular. A typical specular distribution is shown in curve a of Figure 2. The angle of

incidence is usually denoted by an arrow on the abscissa. It is also customary to plot linear signal amplitude as a function of scattering angle although polar plots are sometimes used. In order to compared data from different experiments, the intensities are normalized by dividing by the maximum intensity of the incident beam. In the case where the particles emitted from the surface have completely equilibrated with the surface, one obtains a cosine distribution as shown in curve b of Figure 2.

Finally, Figure 3 shows a molecular beam vacuum system used for scattering studies and incorporating many of the design features and equipment mentioned here.[34]

III. Theories of Beam-Surface Interactions

A. Types of Interactions

When a gaseous particle in a molecular beam collides with a solid surface, it can interact either elastically or inelastically. In an inelastic collision energy exchange occurs, and the interaction results in the creation and/or annihilation of phonons in the solid.[35] In the elastic collision there is no net energy exchange between the gas atom and the solid, and one may see diffraction phenomena. Most of the theoretical work to date has been directed towards interpreting inelastic scattering of monatomic inert gases from solid surfaces using classical models. There have also been quantum mechanical theoretical studies of inelastic scattering. Feuer[36] studied the interaction between rigid rotor diatomics and a

solid surface. There has been essentially no theoretical work done to interpret reactive scattering.

As outlined by Goodman[35] for the inelastic case, there are three possible results of the collision. First, the molecule can lose enough of its energy to become trapped or adsorbed on the surface. Adsorbed molecules will eventually desorb and contribute to the scattered signal. Since these molecules have had a chance to equilibrate with the surface, they are likely to desorb with a cosine spatial distribution and with Maxwellian velocities characteristic of the surface temperature. Second, the molecule can lose some of its energy but still be scattered directly back into the gas phase. It is this second type of inelastic scattering which has received the greatest amount of theoretical attention. As an intermediate third case, the molecule may lose insufficient energy to adsorb but also not scatter immediately. It becomes a "hopping" molecule along the surface.[35]

Different regimes of scattering can be described as a function of the relative values of beam energy and mass and surface atomic mass, temperature and available phonon energies.[35] Associated with these different scattering regimes, different types of theoretical models appear more consistent with experimental observations. Some of the better known classical models and the conditions under which they are applicable are discussed briefly below.

B. Inelastic Scattering

1. "Thermal Scattering" and the Cube Models

The thermal scattering regime is characterized by relatively low incident beam energies and relatively large gas-solid interaction distances (no surface penetration) resulting in scattering from an apparently smooth or flat surface.[35] This regime was first discussed by Oman.[37] In this case, the most important gas-solid interaction mechanism is through the thermal motion of the surface atoms and is most applicable to scattering from metals.[38] Because of the apparently flat surface, the thermal motion that is important during scattering is in the direction normal to the surface.[35]

The theoretical models incorporating a flat surface and only perpendicular surface atom motion are the cube models. The first of these, the "hard cube" model, was developed by Logan and Stickney[39] and is illustrated in Figure 4. The model assumptions are as follows: (1) the intermolecular gas-solid potential is such that the repulsive force is impulsive; (2) the scattering potential is uniform in the plane of the surface (smooth surface), and since there is no motion of surface atoms parallel to the surface, there is no change in the tangential component of the incident particle velocity; (3) surface atoms are represented by independent cubes, and a gas particle interacts with a single surface atom by colliding with the cube once and then being scattered; (4) a temperature-dependent velocity distribution is assigned to the surface atoms. There

is no attractive part to the potential. Referring to Figure 4, the surface atom of mass M_s moves with a perpendicular velocity V_o. A gas molecule of mass M_g strikes the surface cube of mass M_s at an incident angle θ_o (with respect to the surface normal) and with an incident normal velocity V_{no} and a tangential velocity V_{to}. The particle is then scattered at an angle θ_1 with and velocities $V_{t1} = V_{to}$ and V_{n1}. The hard cube problem can be solved exactly, and angular distributions of scattered atoms can be calculated if the velocity distribution of the incident beam is known. The model is somewhat unrealistic in that it neglects the attractive part of the gas-solid potential in the low incident beam energy region where it is most important.[35] The interaction between solid atoms is neglected, and tangential momentum exchange is not considered.

The first two failings are at least partly corrected in the "soft cube" model of Logan and Keck.[40] In this model the assumption of a flat surface is maintained with no exchange of tangential momentum. Now, however, there is a gas atom-solid atom potential with two parts,[40] a stationary attractive part, which increases the normal component of the gas velocity before the repulsive collision and decreases it again afterwards, and an exponential repulsive part. Also, the surface atom involved in the collision is connected by a single spring to a fixed lattice. The ensemble of oscillators making up the surface has an equilibrium distribution of vibrational energies corresponding to the temperature of the solid.[40] This model is shown in Figure 5. The model introduces adjustable parameters for the potential well depth, range of interaction

and lattice atom frequency. The solutions of the equations for angular distributions are approximate. The soft cube model is more successful than the hard cube model at predicting angular distributions for scattering of heavy molecules where potential attractions would be expected to be largest.[40] The model still does not include coupling between atoms of the solid.

2. "Thermal Scattering" and General Three-Dimensional Models

The cube models are only single particle models and only one-dimensional since they are restricted to energy transfer along the momentum component perpendicular to the surface. Classical three-dimensional lattice models have been developed by Oman,[37] Lorenzen and Raff,[41-44] and McClure.[45] In the lattice models an ensemble of lattice points is constructed to correspond to a particular crystal plane. Classical trajectories for scattered molecules are calculated for known incident velocities and angles by solving the equations of motion of the gas molecule and the lattice points. The gas molecule-solid atom potential is assumed to be a pairwise Morse interaction in the work of Lorenzen and Raff and a Lennard-Jones 6-12 potential in the models of Oman and McClure. Such a lattice model is illustrated in Figure 6 in a diagram taken from Goodman.[35] Subscript o refers to incident molecules while 1 refers to reflected molecules. Θ is the Debye temperature of the solid. All surface atoms are connected to nearest neighbors by harmonic springs. In order to obtain reasonably reliable results a large number of trajectories must be calculated, and

the incident trajectories must be chosen so that the distribution in incident angle and energy is both smooth and realistic.[35] Solving the necessary equations for the large number of trajectories needed is difficult and time-consuming and must be done numerically. The recent calculations of McClure[45-48] have been very successful at reproducing experimental results.

3. "Structure Scattering"

In his calculations Oman[37] found that at high incident beam energies new features appeared in his scattered distributions which he atttributed to the incident molecules "seeing" the periodic surface lattice. This is the regime of large incident energies, short interaction distances and a large ratio of incident beam energy to the thermal energy of the solid.[35] The flat surface cube models no longer apply in this regime. One model which has been successfully applied is the hard sphere by Goodman.[49] This model will not be discussed here in detail.

An interesting phenomenon associated with the structure scattering regime is rainbow scattering. This can be viewed as a classical mechanical result of the two-dimensional periodicity of the gas-solid interaction potential.[35] Its origins have been discussed by McClure,[48] and in an extension of his earlier lattice model[45] he has carried out very high resolution (3-5°) calculations of the rainbow scattering of Ne from LiF[47,48] in excellent agreement with experiment. These calculations appear sufficiently reliable

allow
to Λ parameters for the gas-solid potential to be extracted by comparing theory with experiment.[47,48] The calculations are not applicable to gas atom-metal systems.

Since energy can only be exchanged between a gas phase particle and a solid surface through the phonons of the solid, a logical theoretical course is to treat the system quantum mechanically. There has recently been a revival of interest in the quantum theory of gas-solid interactions.[50,51] General inelastic scattering theories based on single phonon interactions have been presented by Manson and Celli,[52] Goodman,[53] and Beeby.[54,55] Ultimately, it is desirable to have a full three-dimensional multi-phonon quantum treatment for a wide range of scattering phenomena. This state has not yet been reached, however.

C. Elastic Scattering

The theoretical description of the elastic phenomenon of particle diffraction is a quantum mechanical problem. Quantum treatments of elastic scattering have been formulated by Tsuchida[56] and by Cabrera et al.[57,58]

An interesting outgrowth of the theoretical calculations for elastic scattering has been the investigation of the absence of diffraction of atomic beams by metals. This has been discussed by Beeby[59] and Weinberg[60] in terms of the Debye-Waller factor. Weinberg[61] has suggested that the intensity of scattered molecules as a function of temperature might be used to calculate gas-solid potential well depths if the surface Debye temperature is known.

IV. Results of Elastic Scattering Studies

A. Diffraction

Atomic beam diffraction is, in principle, a very attractive technique for obtaining accurate surface structural data. Atomic de Broglie wavelengths are in the region of 0.5-1.5 Å, and incident energies can be made quite low (<0.1 eV) so that there is no penetration into the surface, which is a problem associated with Low Energy Electron Diffraction. Similarly, atomic beams might also be very useful in investigations of the structure of adsorbed layers.

Unfortunately, as pointed out by Mason and Williams,[62] atomic beam scattering as a structural probe suffers from the fact that only a small fraction of the total scattering arises from coherent events. This is particularly true for metals where diffraction has been seen only for the relatively "rough" tungsten (112) surface.[63] Efforts by Beeby[59] and Weinberg[60,61] to correlate the lack of diffraction with the magnitude of the Debye-Waller factors have not been successful. It is likely that the absence of diffraction features from metal surfaces is simply due to a much too weak periodicity in the surface potential[62] as experienced by the incoming gas atoms.

Until very recently, only alkali halide crystals had yielded intense, unambiguous diffraction patterns. Atomic diffraction was first seen by Estermann and Stern in 1930[64] from a LiF surface. Subsequently, their results have been reproduced and refined. O'Keefe et al.[65] have reported

that H_2O is a very likely contaminant in their scattering work from LiF(001) and is very possibly a contaminant in previous work. Williams[66,67] in a recent and comprehensive study seems to have successfully cleaned his LiF (001) surface. In one experiment[67] he used a nearly monoenergetic nozzle beam of helium and, his diffraction peaks are listed in Table 1a. The first order peak is about 10% of the intensity of the specular (00) peak, and the second order peak is about 1%, in agreement with theory.[56] The relative intensities seem to be functions of incident beam angle. In a second experiment[66] Williams observed diffraction with a nozzle beam of neon from LiF(100). Figure 7 shows the resulting in-plane diffraction peaks. The total scattered intensity is much weaker than for helium, indicating a greater fraction of inelastic collisions. Also, the higher order peaks are more intense than the lower order peaks, in contrast to the helium results. The weak peaks in the vicinity of the (00) peak are attributed to inelastic scattering from phonons and will be discussed below. The complete diffraction pattern with relative intensities is summarized in Table 1b. Mason and Williams[62] have also examined the diffraction by adsorbed molecules on LiF(001) and found they could obtain diffraction from an ordered overlayer of ethanol and even assign a tentative structure to this layer.

In addition to helium and neon, diffraction has been observed from alkali halide surfaces with H_2 beams and H atoms and marginally with D_2 beams.[65,68,69]

The first observation of atomic beam diffraction from any non-alkali

halide was the work on tungsten carbide by Weinberg and Merrill.[70] Diffraction peaks are well defined with helium and poorly resolved with D_2. The diffraction data are used to deduce a rather carbon-rich surface structure, possibly WC.

The first observation of diffraction by a metal surface was recently reported from clean tungsten (112) by Tendulakar and Stickney.[63] Tungsten (112) is a rather special case, however, since it has an anisotropic surface unit cell consisting of closely packed rows of exposed atoms in the $[11\bar{1}]$ direction separated by open troughs as shown in Figure 8. When the incident beam is directed across the rows, the zeroth and first order diffraction peaks are seen, and their positions agree with predictions. However, no diffraction peaks are observed when the beam is directed parallel to the rows and channels.

B. Scattering of Helium and Other Atomic Beams to Monitor Surface Disorder and Morphology

The helium-metal interaction is almost completely elastic. This is shown by the very narrow specular scattering peaks obtained from clean, well-ordered, single crystal surfaces. In one recent study, Smith and Merrill[15] examined helium scattering from single crystal Pt(111). They observed a specular scattering peak from a smooth, clean surface only slightly wider(7°) than the width of the incident beam (5°). The intensity of scattering at the specular angle was shown to be very sensitive to the amount of ethylene adsorbed on the surface. The specular intensity could

be quantitatively related to ethylene exposures as low as 0.1 Langmuir (1 Langmuir = 10^{-6} torr sec) and thus was a measure of surface coverage. The intensity and shape of the scattered helium peak as probes of surface conditions on Pt(111) were also studied by West and Somorjai.[14] They found large non-specular components due to surface roughness on chemically etched surfaces and on argon ion bombarded surfaces. Surfaces with disordered overlayers of carbon, CO and C_2H_2 gave very non-specular scattering while ordered CO overlayers were more specular although less so than clean, smooth surfaces.

In a study of helium scattering from single crystal Ag(111), Sau and Merrill[8] found that the intensity at the specular angle decreased and the peak width increased as the surface temperature, T_s, increased. This is shown in Figure 9. An increase in beam width is always associated with a decrease in intensity at the maximum. This broadening with increasing T_s is attributed to a "thermal roughening" of the surface which increases as the mean square displacements of vibrating surface atoms increase with higher T_s. There is a decrease in specular intensity and an increase in peak width going from helium scattering from the close-packed fcc (111) face of silver to the more open bcc (110) plane of tungsten and to the still more open fcc (100) face of platinum.[8] These changes in surface structure are slight and microscopic but are still detectable by helium scattering. This technique has also allowed Sau and Merrill[8] to conclude that epitaxially grown silver films are more disordered than conventionally prepared clean single crystal surfaces.

Ollis, et al.[71] used beams of helium and neon as probes of the state of surfaces of molybdenum and rhenium during oxidation. They were able to obtain information on the coverage, binding states and binding energies of oxygen on their surfaces by measuring the intensity of gas atoms scattered specularly.

V. Results of Inelastic Scattering Studies

A. Rare Gas-Metal Systems

When a monatomic gas particle collides inelastically with a metal surface in the absence of chemical interactions, there can be energy transfer between the translational states of the atom and the vibrational states of the lattice. The incident atom can transfer energy into the lattice (phonon creation) or can absorb energy from it (phonon annihilation) and scatter at a higher energy than the incident particle depending on the relative temperatures of the gas molecule and the surface.

In the same paper in which they reported on helium scattering studies, Sau and Merrill[8] also looked at inelastic scattering. Here the scattering is characterized by decreasing peak intensity with increasing θ_i and increasing T_s as seen in Figure 10 for krypton. Also obvious is the non-specular maximum of the scattered peak with the non-specularity increasing with increasing θ_i. For inelastic scattering there is no correlation between scattering intensity and microscopic surface roughness.

The authors also identified an inelastic scattering regime in which

substantial trapping occurs.[8] Here, a significant number of incident atoms lose enough of their energy to become adsorbed. The regime is best illustrated by xenon scattering as shown in Figure 11 indicating large deviations from specularity and a substantial scattering contribution corresponding to a cosine distribution. This cosine component is from desorbed atoms which have equilibrated with the surface. Also typical of this regime is the increase in peak intensity with increasing T_s. This is due to the decreased trapping probability at high temperatures. The number of atoms trapped can be correlated well to the estimated depth of the attractive potential well for various gas-metal systems. It should be noted that these observations of inelastic collisions are in qualitative agreement with the cube models.

Similar results were observed on scattering rare gases from Pt(111)[7] and W(110).[72] In the Pt(111) experiments it was found that if an incident beam temperature of 700°C was used instead of a room temperature beam, the scattered peaks were closer to the specular angle and narrower. This is shown for krypton in Figure 12. There is also a reversal in trend in intensity as a function of T_s. These trends are predicted by the three-dimensional lattice models, and the effect is attributed to a shorter collision time. A trend toward narrower angular distribution and a supra-specular shift in the peak maximum with increasing beam temperature were also observed earlier by Saltsburg and Smith[73] for heavy molecules scattered from Ag(111). Still another investigation by Romney and Anderson[12] using nearly monoenergetic argon nozzle beams with incident energies 0.05 - 5 eV

confirmed the supraspecular shift to about 0.3 eV but then showed a reversal in this trend at higher incident energies with the scattering maximum returning to the specular angle. This return to specular angle is not predicted by the cube models which fail, not surprisingly, at the high incident energy limit. Miller and Subbarao[74] confirmed the above findings and noted that the scattered peak width first decreases with incident energy and then increases again. The energy of the minimum peak width is a function of the gas scattered, being higher for heavier gases.

One of the best ways to analyze the translational energy transfer in an inelastic molecular beam-surface interaction is to measure the velocities of atoms or molecules scattered from a surface for an incident beam of known velocity. To date a few such measurements have been made for monatomic and diatomic gases. Early work by Fisher, Hagena and Wilmoth[75] was carried out using polycrystalline nickel and stainless steel surfaces. Subsequently Yamamoto and Stickney[9] studied the average velocity of argon scattered from single crystal W(110) using the phase-shift technique and a nearly monoenergetic nozzle beam source. Their results are shown in Figure 13. They found that for a given incident velocity (5×10^4 cm sec^{-1}) the average velocity of the scattered gas increased as the angle of incidence increased. Also, the average energy decreased monotonically as a function of scattered angle away from the surface normal for all incident angles. The latter is predicted by the hard cube model as shown by the dashed curves of Figure 13. As noted, there is good

qualitative but poor quantitative agreement. The experiment was also performed at various surface temperatures, and it was found, not surprisingly, that the average velocity of scattered atoms increased as the surface temperature increased.

Recently Subbarao and Miller[20] studied the scattering of neon and argon from epitaxially grown Ag(111) using nozzle beams of various incident velocities. They found that at low energies (0.31 eV and lower) the mean velocities are highest at the surface normal and decrease monotonically towards the surface tangent in agreement with Yamamoto and Stickney.[9] At high incident energy, 1.36 eV, the mean velocity is virtually constant with scattering angle. Their measurements of the thermal spread in the scattered beam show nearly Maxwellian distributions at the surface normal and narrower distributions towards the tangent. At high incident energy the thermal spread appears constant. The scattered beams were all much more nearly Maxwellian than the incident beam. They also found that at high incident beam energies normal momentum transfer becomes less efficient, the scattering becoming more elastic. Also, there is an increase in tangential momentum transfer in agreement with the theory of McClure.[48]

Siekhaus, Schwarz and Olander[26] report a very interesting experiment in which they $\overset{\text{scattered}}{\wedge}$ various thermal beams from pyrolytic graphite at different temperatures and then measured the temperature of the scattered beam. They found that for O_2, D_2, xenon and krypton there was essentially no change in reflected beam temperature, T_r, for large variations in beam

temperature, T_b. Helium and neon beams showed a slight increase in T_r with increasing T_b. A most unusual result is that in several cases T_r was less than both T_b and the surface temperature T_s. As they point out, in a global exchange process this would violate the second law of thermodynamics. They also studied the effect of T_s on T_r for room temperature beams, and these results are shown in Figure 14 for the annealed basal plane of pyrolytic graphite. The data can be fitted to the empirical formula $T_r/T_c = 1 - \exp(-T_s/T_c)$ where T_c is a constant depending only on the incident gas and the nature of the solid surface. The authors suggest[20] that T_c, while only an empirical parameter, does have some characteristics of gas-surface binding energy and does increase with increasing atomic weight of the incident gas. They discuss their result of T_r being virtually independent of T_b and its dependence on T_s in terms of partial trapping, i.e., incident molecules are trapping long enough to uncouple the re-emission process from the incident energy but not long enough to completely equilibrate with the solid.

B. Scattering of Diatomic and Polyatomic Molecules from Metal Surfaces

The case of scattering diatomic or polyatomic molecules from a metal surface is more complicated than for monatomic gases because of the additional possibility that the internal states of the molecule may interact with the vibrational states of the solid. The vibrational levels of most light molecules are at too high energy to be involved in a gas-solid interaction, but the rotational and translational states certainly are

available for interaction with the solid phonons. In a case where the surface temperature is higher than the gas temperature, energy can be transferred from the lattice phonons to the translational or internal states of the molecule. If the gas temperature is higher than the surface temperature, the translational and internal energy levels of the molecule can interact with the lattice modes resulting in phonon creation.

Scattering of diatomic molecules was investigated by Palmer, Saltsburg and Smith[11] who first compared He^3 and He^4 scattering from epitaxial Ag(111) films and found them very similar in specular intensity and peak width. They then scattered H_2, D_2 and HD from the same surface and found that H_2 scattered in a manner very similar to that of helium but that HD and D_2 both gave a very much reduced specular intensity. The results for the hydrogenic molecules are shown in Figure 15. They[11] also looked at the scattering of HD and D_2 as a function of beam temperature, finding the distributions very broad for 80°K beams compared to 300°K and rather more specular at 1500°K than at 300°K. Their results are discussed in terms of the coupling of the lattice phonons with the rotational levels of the hydrogen molecules. For H_2, the lowest rotational transition energy is at 1032 cal/mole. For D_2 this is only 516 cal/mole. The estimated Debye phonon energy in silver is 450 cal/mole, rather close to the D_2 transition energy, while H_2 would certainly need a less probable multi-phonon process to interact. There is also a transition at 516 cal/mole in HD. The conclusion drawn from this analysis[11] is that it should be much easier for D_2 and HD to couple with the lattice via their rotational states than for H_2. This question

of rotational coupling was examined for D_2 on Pt(111) by Smith and Merrill.[6] They found that the fraction of diffuse D_2 scatter increased with increasing surface temperature. Since this is the reverse of the trend for trapping they suggest that this increase in diffuse scatter is due to increased rotational coupling with the more highly excited lattice vibrations. Merrill and coworkers found similar results for D_2 scattered from W(110)[7,2] and most recently for scattering from single crystal Ag(111).[8]

The scattering of diatomic and polyatomic molecules from platinum (100) was studied by West and Somorjai[5] for a variety of surface conditions. They found for NO, CO, N_2, O_2, H_2 and D_2 a broad scattered peak with a maximum at or near the specular angle. All the peaks were rather broad, indicating substantial energy interaction or possibly surface roughness. They noted almost no difference between H_2 and D_2 scattering although broadening due to surface roughness may have hidden any changes due to rotational interactions. The polyatomic molecules CO_2, N_2O, NO_2, C_2H_2, NH_3 and methylenecyclobutane were also examined. For all except NH_3 there was a maximum in intensity very close to the specular angle and again the peaks were rather broad. For NH_3 the distribution was cosine, indicating complete accommodation. Some of the same molecules were scattered from a Pt(100) surface with a graphite overlayer. These results did not differ significantly from those on clean Pt(100).

The absence of complete accommodation for most molecules indicates inefficient energy transfer between the lattice modes and the incident translational energy even though these energies are of the same order of

magnitude.[5] Indeed, it has been suggested by Beebe and Dobrzynsky[76] that inefficient transfer is expected if translational and vibrational energies are nearly equal.

Both CO and acetylene chemisorb on Pt(100) to form rather well ordered overlayers. In the same series of experiments, West and Somorjai[5] also scattered CO from a Pt(100) surface with an ordered layer of CO and scattered C_2H_2 from an ordered layer of C_2H_2. The comparison between acetylene scattered from clean and acetylene covered Pt(100) is shown in Figure 16. For acetylene the distribution is very nearly cosine. For CO the distribution is very broad, and its maximum does not shift as the incident angle is changed. Both examples indicate nearly complete energy accommodation.

It is possible that when gases such as CO or acetylene are adsorbed, new vibrational modes exist which do allow efficient energy transfer with the incident CO and acetylene gas molecules.[5] It is also pointed out that for these rather heavy molecules with low energy rotational transitions, it is likely that considerable interaction is taking place between the lattice phonons and the rotational states. There could also be transfer of rotational energy into translational energy of the gas molecule.

In other work on polyatomic molecular scattering Saltsburg and Smith[73] looked at CH_4 and NH_3 scattered from Ag(111) films and found also that NH_3 has a cosine distribution and CH_4 is highly non-specular although non-cosine. Also, Saltsburg, Smith and Palmer[77] scattered CO_2, CO, O_2, N_2, H_2, D_2 and HD from Ag(111) films, finding broad peaks at or near the specular angle in all cases.

C. Direct Observation of Phonon Interaction

In the papers in which high resolution helium and neon diffraction was reported, Williams[66,67] also reported small peaks in the vicinity of the specular peak which he attributed to direct phonon interaction. These peaks are seen in Figure 7 for neon. Both phonon absorption and emission are seen. From his data on helium and an assumption of surface phonons only, he was able to calculate a dispersion relationship. Fisher and Bledsoe[78] scattered 0.058 eV helium from LiF(001) and analyzed the scattered velocity distributions, also finding peaks they assigned to single phonon absorptions and emissions, with emissions dominating.

In a study of very low energy helium scattering from a Ag(111) film, Subbarao and Miller[79] observed a peak in the angular distribution which they attribute to inelastic scattering from lattice phonons. The results are shown in Figure 17. The position of the peak maximum is a function of the incident beam velocity while the specular peak width remains constant. Recently, Subbarao and Miller[80] have expanded this work on helium on Ag(111) and come to the conclusion that the interaction involves bulk phonons only.

VI. Reactive Scattering of Molecular Beams

How is the energy of a chemical surface reaction distributed among the reactants and the products? This is one of the fundamental questions of surface science, and it appears that the technique of reactive scattering

of molecular beams can provide the answer. To demonstrate this let us consider a relatively simple surface reaction, the recombination of hydrogen atoms on a metal surface. The hydrogen atoms emanate from a high temperature source (greater than 2000°K) and have kinetic energy corresponding to the source temperature. As the hydrogen atoms impinge on the surface that is held at a lower temperature, some of their translational energy is transferred to the solid through lattice vibrations (T-V energy transfer), and many of the atoms become trapped on the surface. As a result of surface diffusion, there is a high probability of recombination of the adsorbed atoms that is in general a highly exothermic reaction (over 100 kcal for hydrogen). The reaction energy is then partitioned between the solid and the desorbing molecules. By measuring the velocity of the desorbing molecules and their angular distribution, the distribution of chemical energy can be determined.

If the molecules stay on the surface long enough after the chemical reaction, they can come to equilibrium with the surface. In this circumstance, the desorbing molecular beam will have a cosine angular distribution and an average "translational" temperature that is equal to the surface temperature. A non-cosine angular distribution and/or a higher translational energy than expected based on the surface temperature would indicate poor thermal equilibrium and that a portion of the chemical energy is converted to translational energy of the scattered molecules. If the desorbing molecules carry with them much of the energy of the chemical reaction, they may be in an excited rotational, vibrational or electronic

state in addition to having increased kinetic energy. The partitioning of chemical energy between internal modes of the molecules and their translational energy is another important question that can be answered by molecular beam scattering studies utilizing measurements of the velocity of the reaction product and their angular distribution. So far, such detailed measurements of energy partitioning in surface chemical reactions have not been made although the experimental techniques that have been developed in various laboratories recently can provide such information. No doubt, investigations of this type will be carried out in the near future.

We shall now review the reactive scattering studies that have been carried out so far using molecular beams and clean solid surfaces. These reactive scattering studies may be divided into two classes: (A) chemical reactions where the surface acts as a catalyst for dissociation or recombination of the reactant molecules and (B) those in which the surface is one of the reactants.

A. Catalytic Surface Reactions

The hydrogen-deuterium exchange reaction, $H_2 + D_2 = 2HD$ has been studied by Saltsburg et al.[81] on epitaxially grown nickel surfaces with (111) orientation. The angular distribution of HD was $\cos^3 \theta$ instead of $\cos \theta$ indicating incomplete accommodation of the reaction product with the surface. It was argued that HD molecules formed only when an H atom and a D atom were in close proximity and evaporated coherently to explain the angular dependence that was observed. The H_2-D_2 exchange reaction

was studied by Bernasek et al.[34] using platinum single crystal surfaces. No HD signal was detected on scattering a mixed hydrogen-deuterium beam from the (111) crystal face. However, when the diatomic molecules were scattered from a stepped high Miller index platinum surface, 5-10% HD product was detectable. High Miller index single crystal surfaces are characterized by ordered arrangement of atomic steps one atom high separated by terraces of low Miller index orientation. In their study the terraces were 9 atoms wide and of (111) orientation. The observed H_2, D_2 and HD scattering distributions from the (111) and the stepped platinum surface are shown in Figure 18. This study has shown that atomic steps play an all important role in dissociating large binding energy diatomic molecules. Chopping the incident beam to generate an ac signal was used to obtain a better signal-to-noise ratio and to measure surface residence times by the phase shift technique. Varying the chopping frequency has yielded HD residence times of 25 milliseconds on a stepped platinum surface at a 700°K surface temperature. Such a long residence time should result in complete thermal equilibration between the surface and the reaction products. This was found by experiments as the desorbing HD beam exhibited cosine angular distribution.

Reactive scattering studies with two or more reactants can be carried out either using a mixed molecular beam or by preadsorbing one of the reactants on the surface and monitoring the reaction between one of the reactants in the molecular beam and the other reactant that was adsorbed. Although detailed comparison between the two modes of reactions have not

been made as yet, it is likely that the surface reaction kinetics may change as the reaction conditions are varied in this manner.

The dissociation of H_2 on tungsten surfaces was studied by Smith and Fite.[82] The reaction probability increased to 0.3 above 3000°K. The angular distribution of H atoms was cosine-like indicating thermal equilibration between the hot surface and the desorbing H atoms. This was also corroborated by a long residence time, 280 μsec, that was measured. The dissociation of H_2 on tantalum surfaces was studied by Krakowski et al.[83] in the temperature range of 1100-2600°K. The reaction probability increased with increasing temperature just as for tungsten surfaces. The hydrogen atoms underwent complete thermal accommodation on the surface. By varying the kinetic energy ("beam temperature") of the incident beam they have determined an activation energy of 1.4 kcal/mole for the atomization surface reaction. Thus, the atoms once formed cannot undergo recombination before desorption from the hot surface. The rate limiting step in the reaction appears to be the desorption of H atoms which has an activation energy of about 75 kcal/mole. The surface diffusion of H atoms does not require activation energy.

The dissociation of N_2O on hot tungsten has been investigated by Muschlitz.[84] The decomposition probability approaches unity at high surface temperatures. The product N_2 was emitted with a cosine distribution while neither oxygen atoms nor oxygen molecules could be detected in the scattered beam. It appears that oxygen reacts with the tungsten surface during the decomposition of N_2O. Both N_2 and NO were found in the

scattered beam and the ratio of the two species, N_2/NO, was approximately 12:1 at 2500°K. During the dissociation of N_2O on platinum surfaces that was studied by West and Somorjai[85] again both NO and N_2 were found, the NO concentration being larger than that found on desorption from tungsten surfaces. The angular distribution of the product NO molecule that formed by dissociation at the clean platinum surface was of the cosine type indicating complete accommodation of the NO molecule on the surface prior to re-emission. The angular distribution of NO product molecules is quite different, however, when they are emitted from carbon covered platinum surfaces at 1125°K. The angular distribution is certainly non-cosine, and it peaks at or near the specular angle. Such a peaked spatial distribution reflects a lack of energy accommodation during the surface dissociation reaction of N_2O on the carbon covered platinum (100) surface and suggests a direct reactive scattering mechanism. N_2O may undergo a variety of chemical reactions on platinum and carbon covered platinum surfaces. Those chemical reactions that can take place between the carbon on the platinum surface and N_2O are largely exothermic and yield CN, CO or CO_2 reaction products in addition to N_2 and NO. On the clean platinum surface where the incident N_2O molecules can only undergo endothermic chemical reactions. In this case the dissociated species appear to be fully accommodated on the surface before re-emission as indicated by the cosine angular distribution of the scattered beam. On the carbon

covered platinum (100) surface where surface reactions can be strongly exothermic, there is evidence for direct reactive scattering, and NO molecules are emitted without complete energy accommodation between the incident beam and the surface as indicated by the non-cosine angular distribution of the scattered beam. Direct scattering is commonly observed in studies of chemical reactions between crossed molecular beams that are exothermic and exoergic.

The chemical reaction between deuterium and oxygen to form D_2O occurring on the (111) platinum surface has been investigated by Smith and Palmer.[86] In these studies the molecular beam was D_2, and the oxygen was preadsorbed on the platinum surface which was maintained in an oxygen ambient. The production of D_2O was studied as a function of D_2 flux and temperature, oxygen pressure, platinum surface temperature, and angle of incidence of the D_2 beam. It was found that the reaction rate is proportional to the second power of the D_2 pressure and the 0.8 power of the oxygen pressure. The adsorption of D_2 requires an activation energy of 1.8 kcal/mole. It is proposed that in the adsorbed state the reaction proceeds upon the collision of 4 adsorbed deuterium atoms with an adsorbed oxygen molecule or activated oxygen complex.

Nutt and Kapur[87] reported on preliminary experiments involving the oxidation of ammonia using NH_3 and O_2 mixed molecular beams. The reaction products were N_2, H_2O and NO in the temperature range of 600-1200°K, and the reaction probability was about 0.1-0.2.

on silver surfaces

The oxidation of C_2H_4 was studied by Smith et al.[88] They found no evidence for the formation of ethylene oxide, CO_2 being the dominant reaction product. The surface temperature dependence of the CO_2 formation indicated an activation energy of 8 kcal/mole. The reaction probability was less than 10^{-2} at 820°K, and poisoning of the surface reaction by carbon that builds up on the silver surface was inferred from the experimental data. The hydrogenation of ethylene was studied using the (111) crystal face of platinum.[89] The reaction probability can be estimated to be about 10^{-4} in the range of 500-700°C. As a result, the formation of ethane could not be detected.

Olander et al.[29,90] have studied the oxidation of both the basal plane and the prism plane of graphite. The product of the oxidation reaction is CO although a small CO_2 signal was also detectable during oxidation of the prism plane. The reaction rate was monitored as a function of surface temperature. From the chopping frequency dependence of the reaction probability they have concluded that there must be at least two parallel reactions, one slow and one faster, taking place on the graphite surface. For the basal plane the faster reaction is attributed to the migration of atomic oxygen over the surface to reaction sites where oxidation occurs. The rate constant, k, for this step is given by $k = 2.5 \times 10^{7} \exp(-30 \text{ kcal/RT}) \text{ sec}^{-1}$. The slower reaction step is the desorption of CO, and its rate constant, k_d, is given by $k_d = 3 \times 10^{12} \exp(-50 \text{ kcal/RT}) \text{ sec}^{-1}$. There are two types of reaction sites postulated with surface concentrations of 10^{11} cm^{-2} and 10^{8} cm^{-2}, respectively. Grain boundary and possible bulk

diffusion of oxygen was found to be an important step in the oxidation of the prism face.

B. Reactions Between Gases and Solid Surfaces

The interaction between chlorine molecular beams and nickel surfaces has been studied by McKinley[91] and Smith and Fite.[92] The reaction probability is 0.8 at 1000°K, and both NiCl and $NiCl_2$ are detectable among the reaction products. The formation of NiCl predominates at low temperatures while $NiCl_2$ forms almost exclusively above 1400°K. The mechanism that is proposed involves a Ni_2Cl_2 surface intermediate. The formation of this dimer appears to be the rate limiting step in the overall reaction while the desorption of NiCl and $NiCl_2$ are rapid reaction steps. The residence time of the desorbing NiCl is 916 μsec at 1150°C and 140 μsec at 1300°C, and the NiCl residence times are even longer. The oxidation of germanium was studied by Anderson and Boudart[93] and Maddix and Boudart.[94] The reaction probability was 0.04 and independent of temperature. However, the oxidation rate of the surface was dependent on the oxygen beam temperature which indicates 100-200 cal/mole activation energy for the adsorption. It appears that the dissociative adsorption of oxygen is the rate determining step in the reaction. The oxidation reaction using oxygen atoms instead of oxygen molecules was also investigated.[95] The reaction probabilities in this case are in the range of 0.2-0.3, much higher than for oxygen molecules for surface temperatures in the range of 830-1110°K. The difference in reactivities appears to be due to the

requirement that both atoms in the oxygen molecule interact simultaneously with the surface atom. Thus, the interaction probability depends on the orientation criterion.

Some of the surface reactions that have been studied were endothermic (the decomposition of N_2O, for example) while others were exothermic (oxidation reactions, etc.). It should be noted that only exothermic reactions are likely to yield reaction products with excess translational or internal energy because in this circumstance surplus chemical energy is available to the desorbing molecules. During endothermic reactions the reaction products are likely to thermally equilibrate with the surface and then desorb with a cosine spatial distribution and without excess translational or internal energy.

VII. Future Trends

The field of molecular beam-surface scattering is one of the frontier areas of surface science. The energy transfer that takes place in surface reactions between the gas and the surface atom is the key to understanding the reactivity of surfaces. Therefore, this field will be growing rapidly over the next decade, we believe. There are many areas of development that can be identified already. Improvements in experimental techniques will permit the investigator to use single crystal surfaces and to monitor the velocity of the scattered products as well as their angular distributions. Perhaps the velocity of the scattered beam is a more important experimental parameter in understanding energy transfer than the

angular distribution of the emitted beam. The use of single crystal surfaces of well defined structure permits studies of the correlation between gas-surface energy transfer and surface structure to explore the effects of atomic steps, the variation of atomic spacing and the structure of the adsorbed layer. Nozzle beam techniques will allow the use of more monochromatic molecular beams of higher intensity with corresponding improvements in measurements of residence times of adsorbed molecules, intensities of the emitted beams and their times of flight.

There are various types of energy transfer processes that can take place between the incident gas and the surface that involve T-V, R-V, V-V and other types of energy transfer processes as mentioned in this chapter. Experiments can be devised that will separate these various processes and study the transition probabilities of each. The important question of how the total energy of the collision partners is distributed among the surface atom and the translational and internal energy modes of the emitted particles will then be answered.

One of the important areas of the molecular beam surface scattering field is the study of beams of condensible vapors as they interact with surfaces. There are several laboratories where research in this area has been initiated recently, and there is a great number of interesting problems that may be solved by this technique. Problems of crystal growth from the vapor, surface diffusion mechanisms, and energy transfer during condensation and nucleation can be studied this way.

Reactive scattering of molecular beams promises to shed light on

the elementary steps of surface reactions. This field is just beginning to attract a great deal of interest and will be growing rapidly during the next decade. Molecular beam surface scattering studies are likely to answer many important scientific and technical problems in the fields of surface science, heterogeneous catalysis, aerospace sciences and astrophysics.

Acknowledgement

This work carried out under the auspices of the U. S. Atomic Energy Commission.

References

1. Fundamentals of Gas-Surface Interactions, H. Saltsburg, J. N. Smith and M. Rogers, Editors (Academic Press, New York, 1967).
2. R. E. Stickney, in Advances in Atomic and Molecular Physics, D. R. Bates and I. Estermann, Editors (Academic Press, New York, 1967), p. 143.
3. J. P. Toennies, To be published.
4. R. P. Merrill, Cat. Rev. 4, 115 (1970).
5. L. A. West and G. A. Somorjai, J. Chem. Phys. 57, 5143 (1972).
6. D. L. Smith and R. P. Merrill, J. Chem. Phys. 53, 3588 (1970).
7. A. G. Stoll, D. L. Smith and R. P. Merrill, J. Chem. Phys. 54, 163 (1971).
8. R. Sau and R. P. Merrill, Surf. Sci. 34, 268 (1973).
9. S. Yamamoto and R. E. Stickney, J. Chem. Phys. 53, 1594 (1970).
10. J. N. Smith and H. Saltsburg, J. Chem. Phys. 40, 3584 (1964).
11. R. L. Palmer, H. Saltsburg and J. N. Smith, J. Chem. Phys. 50, 4661 (1969).
12. M. J. Romney and J. B. Anderson, J. Chem. Phys. 51, 2490 (1969).
13. R. L. Palmer, J. N. Smith, H. Saltsburg and D. R. O'Keefe, J. Chem. Phys. 53, 1666 (1970).
14. L. A. West and G. A. Somorjai, J. Chem. Phys. 54, 2864 (1971).
15. D. L. Smith and R. P. Merrill, J. Chem. Phys. 52, 5861 (1970).
16. J. B. Anderson, R. P. Andres and J. B. Fenn, in Advances in Chemical Physics, Vol. 10, J. Ross, Editor (John Wiley & Sons, New York, 1966) p. 275.
17. R. J. Gordon, Y. T. Lee and D. R. Herschbach, J. Chem. Phys. 54, 2393 (1971).
18. W. J. Hays, W. E. Rodgers and E. L. Knuth, J. Chem. Phys. 56, 1652 (1972).
19. T. R. Dyke, G. R. Tomasevich, W. Klemperer and W. E. Falconer, J. Chem. Phys. 57, 2277 (1972).

20. R. B. Subbarao and D. R. Miller, J. Chem. Phys. 58, 5247 (1973).

21. R. H. Jones, D. R. Olander and V. Kruger, J. Appl. Phys. 40, 4641 (1969).

22. D. R. Olander, J. Appl. Phys. 40, 4650 (1969).

23. W. J. Siekhaus, R. H. Jones and D. R. Olander, J. Appl. Phys. 41, 4392 (1970).

24. D. R. Olander and V. Kruger, J. Appl. Phys. 41, 2769 (1970).

25. H. Harrison, D. G. Hummer and W. L. Fite, J. Chem. Phys. 41, 2567 (1964).

26. W. J. Siekhaus, J. A. Schwarz and D. R. Olander, Surf. Sci. 33, 445 (1972).

27. S. Yamamoto and R. E. Stickney, J. Chem. Phys. 47, 1091 (1967).

28. R. H. Jones, D. R. Olander, W. J. Siekhaus and J. A. Schwarz, J. Vac. Sci. & Tech. 9, 1429 (1972).

29. D. R. Olander, W. J. Siekhaus, R. Jones and J. A. Schwarz, J. Chem. Phys. 57, 408 (1972).

30. R. J. Madix and J. A. Schwarz, Surf. Sci. 24, 264 (1971).

31. A. E. Dabiri, T. J. Lee and R. E. Stickney, Surf. Sci. 26, 522 (1971).

32. O. F. Hagena, Appl. Phys. Lett. 9, 385 (1966).

33. K. Kodera et al., Japan. J. Appl. Phys. 10, 543 (1971).

34. S. L. Bernasek, W. J. Siekhaus and G. A. Somorjai, Phys. Rev. Lett. 30, 1202 (1973).

35. F. O. Goodman, Surf. Sci. 26 327 (1971).

36. P. Feuer, J. Chem. Phys. 1131 (1963).

37. R. A. Oman, J. Chem. Phys. 48, 3919 (1968).

38. J. N. Smith, H. Saltsburg and R. I. Palmer, J. Chem. Phys. 49, 1287 (1968).

39. R. M. Logan and R. E. Stickney, J. Chem. Phys. 44, 195 (1966).

40. R. M. Logan and J. C. Keck, J. Chem. Phys. 49, 860 (1968).

41. J. Lorenzen and L. M. Raff, J. Chem. Phys. 49, 1165 (1968).

42. J. Lorenzen and L. M. Raff, J. Chem. Phys. 52, 1133 (1970).

43. J. Lorenzen and L. M. Raff, J. Chem. Phys. 52, 6134 (1970).

44. J. Lorenzen and L. M. Raff, J. Chem. Phys. 54, 674 (1971).

45. J. D. McClure, J. Chem. Phys. 51, 1687 (1969).

46. J. D. McClure, J. Chem. Phys. 57, 2810 (1972).

47. J. D. McClure, J. Chem. Phys. 57, 2823 (1972).

48. J. D. McClure, J. Chem. Phys. 52, 2712 (1970).

49. F. O. Goodman, Surf. Sci. 7, 391 (1967).

50. F. O. Goodman, Surf. Sci. 24, 667 (1971).

51. F. O. Goodman and J. D. Gillerlain, J. Chem. Phys. 57, 3645 (1972).

52. R. Manson and V. Celli, Surf. Sci. 24, 495 (1971).

53. F. O. Goodman, Surf. Sci. 30, 1 (1972).

54. J. L. Beebe, J. Physics C 5, 3438 (1972).

55. J. L. Beebe, J. Physics C 5, 3457 (1972).

56. A. Tsuchida, Surf. Sci. 14, 375 (1969).

57. N. Cabrera, V. Celli, F. O. Goodman and R. Manson, Surf. Sci. 19, 67 (1970).

58. N. Cabrera, V. Celli and R. Manson, Phys. Rev. Lett. 22, 346 (1969).

59. J. L. Beebe, J. Physics C 4, L395 (1971).

60. W. H. Weinberg, J. Physics C 5, 2093 (1972).

61. W. H. Weinberg, J. Chem. Phys. 57, 5463 (1972).

62. B. F. Mason and B. R. Williams, J. Chem. Phys. 56, 1895 (1972).

63. D. V. Tendulkar and R. E. Stickney, Surf. Sci. 27, 516 (1971).

64. I. Estermann and O. Stern, Z. Physik 61, 95 (1930).

65. D. R. O'Keefe, J. N. Smith, R. L. Palmer and H. Saltsburg, J. Chem. Phys. 52, 4447 (1970).

66. B. R. Williams, J. Chem. Phys. 55, 1315 (1971).

67. B. R. Williams, J. Chem. Phys. 55, 3220 (1971).

68. D. R. O'Keefe, J. N. Smith, R. L. Palmer and H. Saltsburg, Surf. Sci. 20, 27 (1970).

69. H. Hoinkes, H. Nahr and H. Wilsch, Surf. Sci. 30, 363 (1972).

70. W. H. Weinberg and R. P. Merrill, J. Chem. Phys. 56, 2893 (1972).

71. D. F. Ollis, H. G. Lintz, A. Pentenero and A. Cassuto, Surf. Sci. 26, 21 (1971).

72. W. H. Weinberg and R. P. Merrill, J. Chem. Phys. 56, 2881 (1972).

73. H. Saltsburg and J. N Smith, J. Chem. Phys. 45, 2175 (1966).

74. D. R. Miller and R. B. Subbarao, J. Chem. Phys. 52, 425 (1970).

75. S. S. Fisher, O. F. Hagena and R. G. Wilmoth, J. Chem. Phys. 49, 1562 (1968).

76. J. L. Beebe and L. Dobrzynski, J. Physics C 4, 1 (1971).

77. H. Saltsburg, J. N. Smith and R. L. Palmer, in The Structure and Chemistry of Solid Surfaces, G. A. Somorjai, Editor (John Wiley & Sons, New York, 1969), p. 42-1.

78. S. S. Fisher and J. R. Bledsoe, J. Vac. Sci. & Tech. 9, 814 (1972).

79. R. B. Subbarao and D. R. Miller, J. Chem. Phys. 51, 4679 (1969).

80. R. B. Subbarao and D. R. Miller, J. Vac. Sci. & Tech. 9, 808 (1972).

81. H. Saltsburg, J. N. Smith and R. L. Palmer, presented at New Mexico Sect., Am. Vac. Soc. Symp., "Surface Science, Evaporation and Effusion," Los Alamos, New Mexico, April, 1969.

83. R. A. Krakowski and D. R. Olander, J. Chem. Phys. 49, 5027 (1968).

84. R. N. Coltharp, J. T. Scott and E. E. Muschlitz, in Structure and Chemistry of Solid Surfaces, G. A. Somorjai, Editor (John Wiley & Sons, New York, 1969), p. 66-1.

85. L. A. West and G. A. Somorjai, J. Vac. Sci. & Tech. 9, 668 (1972).

86. J. N. Smith and R. L. Palmer, J. Chem. Phys. 56, 13 (1972).

87. C. W. Nutt and S. Kapur, Nature 220, 697 (1968).

88. J. N. Smith, R. L. Palmer and D. A. Vroom, J. Vac. Sci. & Tech. 10, 373 (1973).

89. D. L. Smith, Ph.D. Thesis, Dept. of Chem. Eng., Univ. of California, Berkeley, 1969.

90. D. R. Olander, R. H. Jones, J. A. Schwarz and W. J. Siekhaus, J. Chem. Phys. 57, 421 (1972).

91. J. D. McKinley, J. Chem. Phys. 40, 120 (1964).

92. J. N. Smith and W. L. Fite, in 3rd Intl. Symp. on Rarefied Gas Dynamics, J. A. Lauramann, Editor (Academic Press, New York, 1963), p. 430.

93. J. Anderson and M. Boudart, J. Catalysis 13, 216 (1964).

94. R. J. Madix and M. Boudart, J. Catalysis 7, 240 (1967).

95. R. J. Madix and A. A. Sasu, Surf. Sci. 20, 377 (1970).

Figure Captions

Figure 1 Block diagram of a molecular beam-surface vacuum system.

Figure 2 Curve a: Angular distribution of highly specularly scattered beam. Arrow indicates angle of incidence.

Curve b: Scattered beam with cosine angular distribution.

Figure 3 Molecular beam-surface scattering apparatus.[34]

Figure 4 The "hard cube" model.[35]

Figure 5 The "soft cube" model.[35]

Figure 6 A three-dimensional lattice model.[35]

Figure 7 In-plane scattering of neon atoms from LiF(100) showing peaks due to diffraction and phonon absorption and emission.[66]

Figure 8 Atomic structure of the (112) face of tungsten.[63]

Figure 9 Angular distribution of helium scattered from Ag(111) single crystal as a function of surface temperature.[8]

Figure 10 Angular distribution of krypton scattered from Ag(111) single crystal as a function of surface temperature (top) and incident angle (bottom).[8]

Figure 11 Angular distribution of xenon scattered from Ag(111) single crystal as a function of surface temperature (left) and incident angle (right).[8]

Figure 12 Angular distribution of krypton scattered from Pt(111) at beam temperature of 23°C (top) and 700°C beam (bottom).[7]

Figure 13 Average velocity of argon atoms scattered from W(110) single crystal as a function of scattered angle for various incident angles. Arrow indicates U_i, the incident velocity, and U_s, the velocity the atoms would have if completely accommodated. The dashed lines show the predictions of the hard cube model.[9]

Figure 14 Temperatures of atoms scattered from the annealed basal plane of pyrolytic graphite as a function of surface temperature. Beam temperature is 27°C.[26]

Figure 15 Angular distributions of hydrogenic molecules from epitaxially grown Ag(111). Surface temperature = 570°K. Beam temperature = 300°K.[11]

Figure 16 Angular distribution of acetylene scattered from clean Pt(100) (top) and acetylene covered Pt(100) single crystals (bottom).[5]

Figure 17 Angular distributions of helium scattered from epitaxially grown Ag(111) for various incident beam temperatures. Surface temperature = 560°K.[79]

Figure 18 Left-hand side: Angular distribution of H_2 and D_2 scattered from Pt(111) single crystal. Right-hand side: Angular distribution of H_2, D_2 and HD scattered from a stepped Pt single crystal. Schematic diagrams of the surfaces are shown above the figures. The HD distribution is shown with scale expanded.[34]

Table I

(a) Approximate Relative Intensities of the Observed Diffraction Peaks for He/LiF[67]

(00)	178	(-1-1)	15	(1-1)	3.1	(2-2)	2.5
(0-1)	16	(-1-2)	1.6	(1-2)	0.6	(2-4)	
(0-2)	1.4	(-1-3)	0.3	(1-3)	0.07		
(0-3)	0.05	(-2-2)	1.2				

(b) Approximate Relative Intensities of the Observed Diffraction peaks for Ne/LiF[66]

(00)	30	(-1-1)	2.5	(-3-3)	11
		(0-1)	14		
(+1-1)	21	(0-2)	50	(-4-4)	9
		(0-4)	10		
(+2-2)	20	(2-4)	8		
		(-1-3)	11		
(+3-3)	4	(-2-2)	2.5		

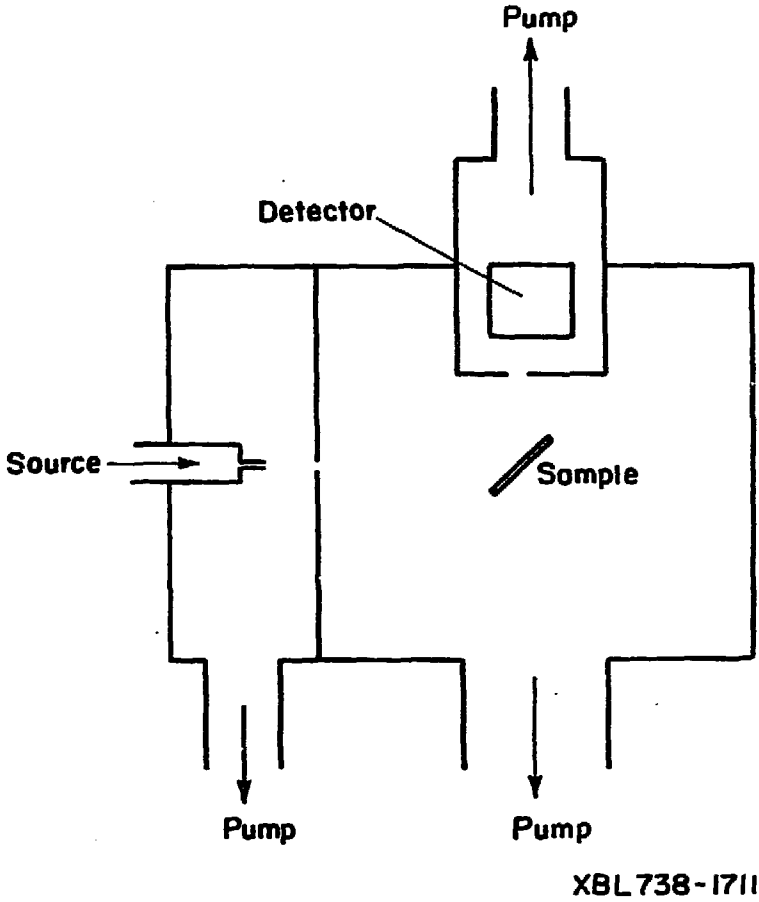

Fig. 1

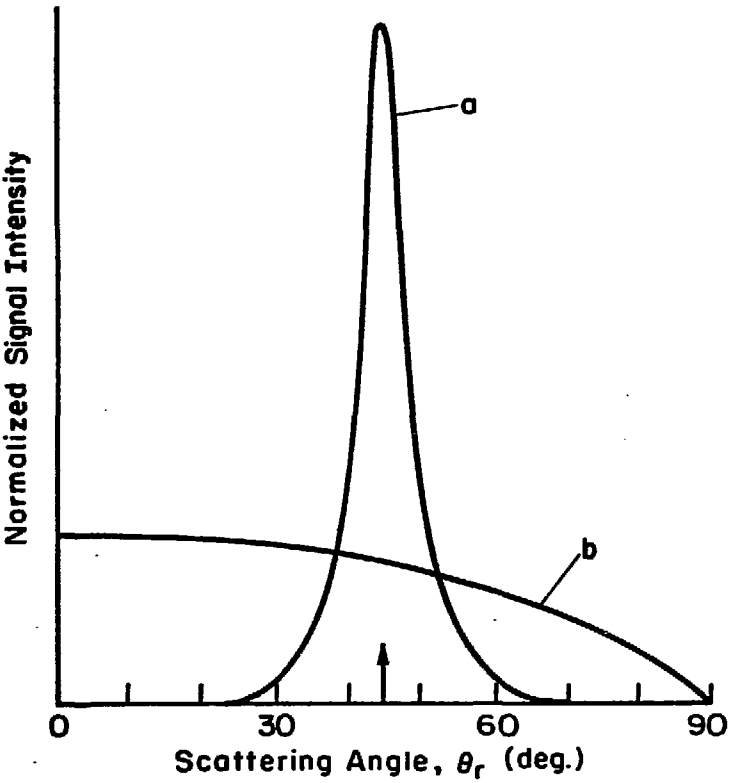
Normalized Signal Intensity
a
b
0
30
60
90
Scattering Angle, θ_r (deg.)
XBL 738-1710

Fig. 2

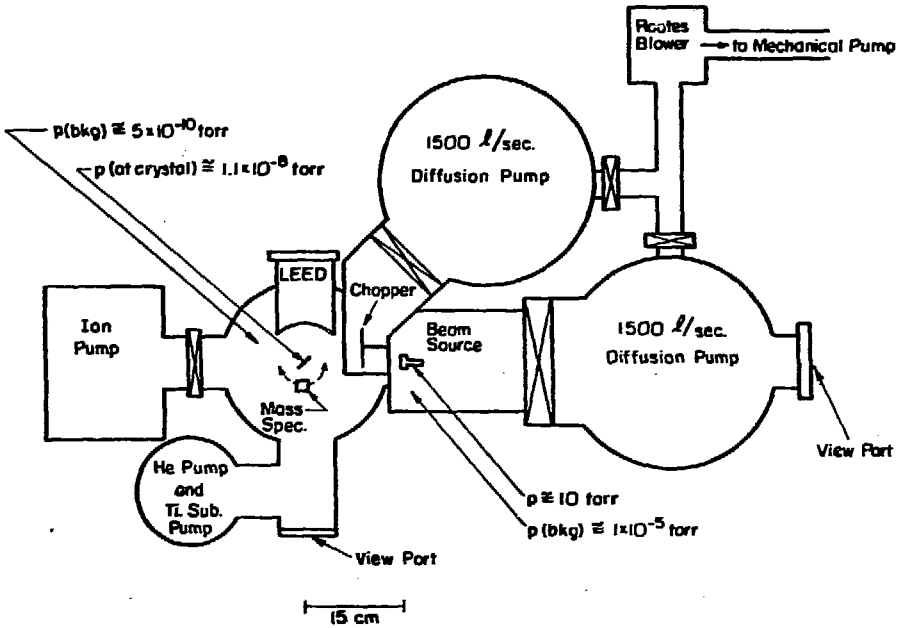

MOLECULAR BEAM SURFACE SCATTERING APPARATUS

XBL 732-5744

Fig. 3

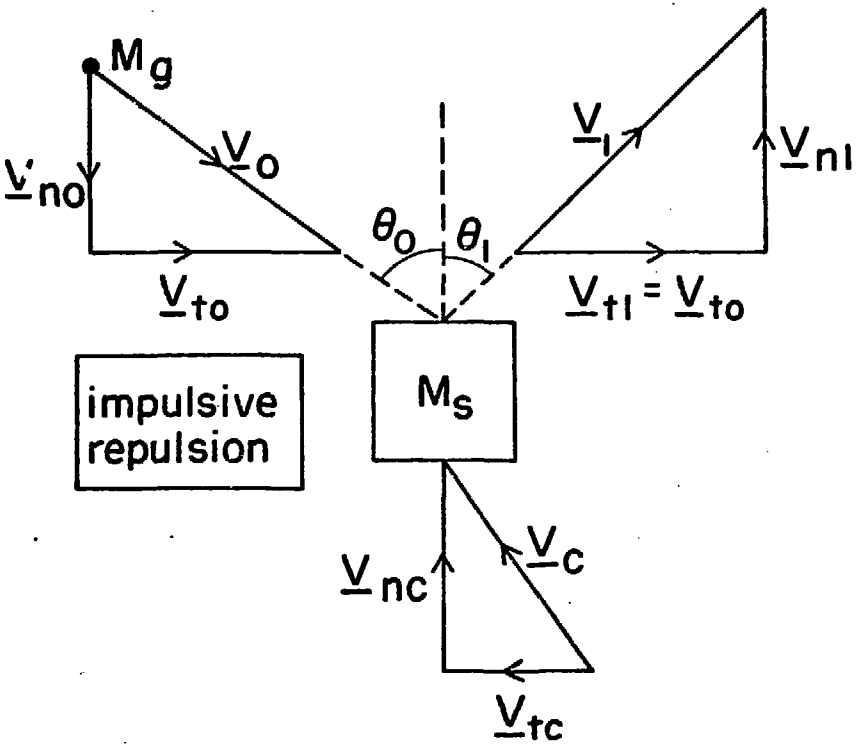

XBL 738-1060

Fig. 4

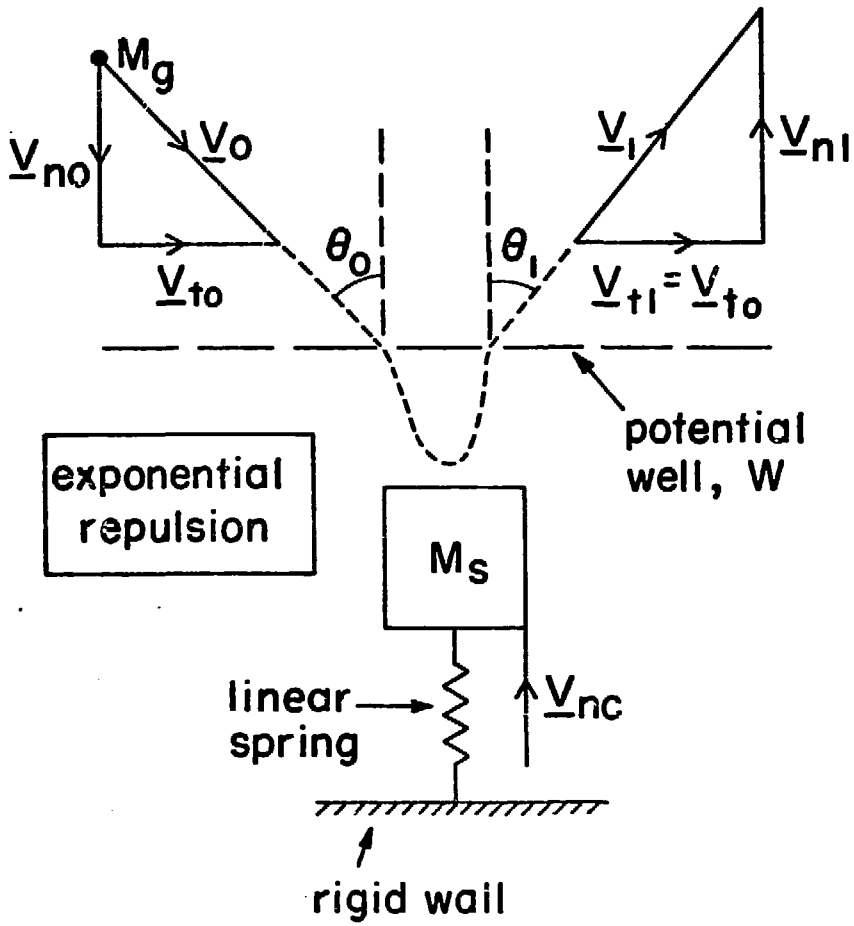
M_g
$\underline{V}_{no}$
$\underline{V}_o$
$\underline{V}_{to}$
θ_o
θ_i
$\underline{V}_i$
$\underline{V}_{ni}$
$\underline{V}_{ti} = \underline{V}_{to}$
potential well, W
exponential repulsion
M_s
linear spring
$\underline{V}_{nc}$
rigid wall
XBL 738-1062

Fig. 5

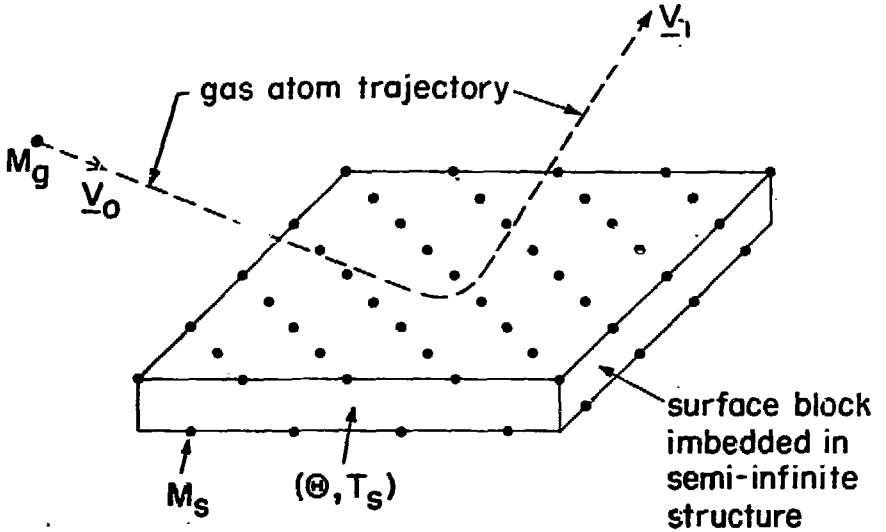

solid atoms are either independent oscillators or oscillators coupled with "springs"

XBL 738-1056

Fig. 6

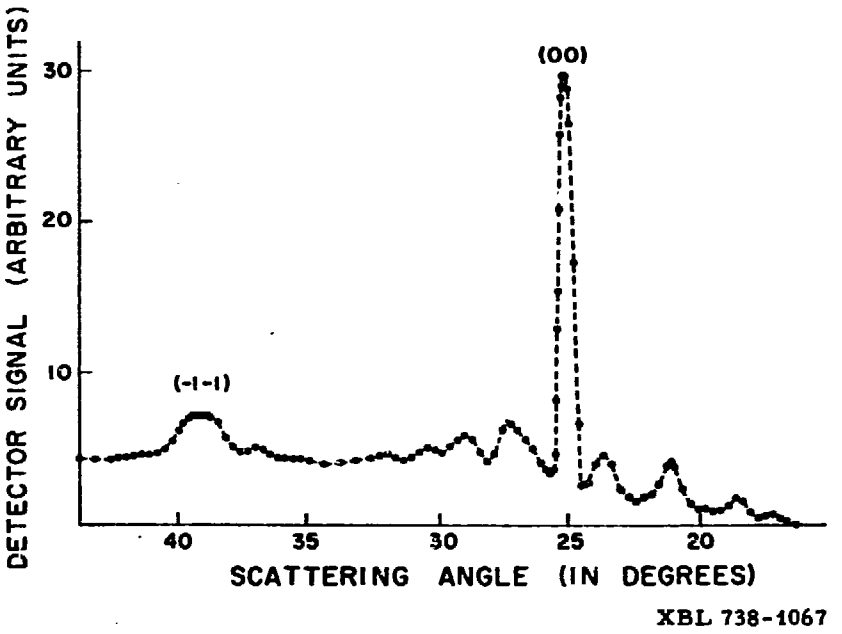
DETECTOR SIGNAL (ARBITRARY UNITS)
30
20
10
(00)
(-1-1)
40
35
30
25
20
SCATTERING ANGLE (IN DEGREES)
XBL 738-1067

Fig. 7

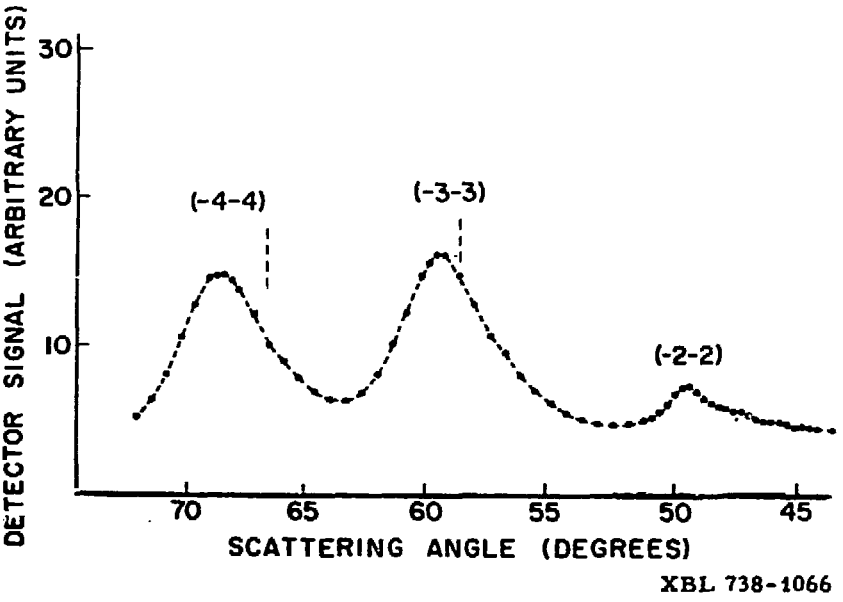

Fig. 7 continued.

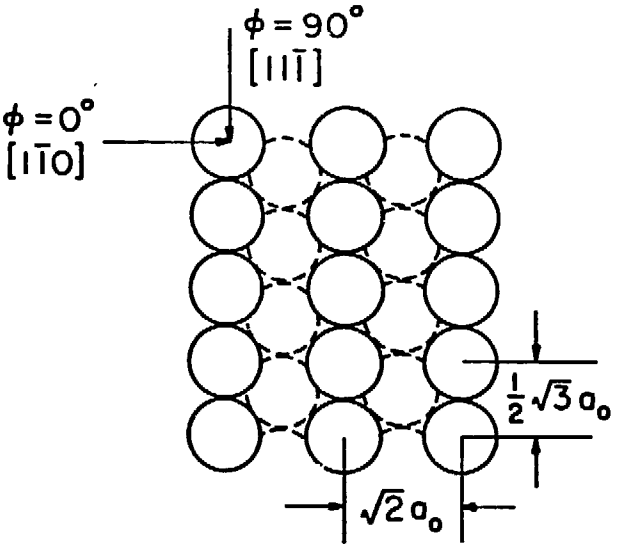

(a)
TOP VIEW
$a_o = 3.16$ Å

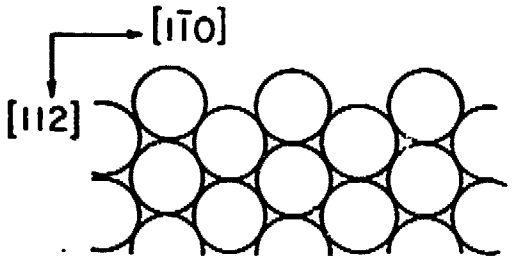

(b)
SIDE VIEW

XBL 738-1059

Fig. 8

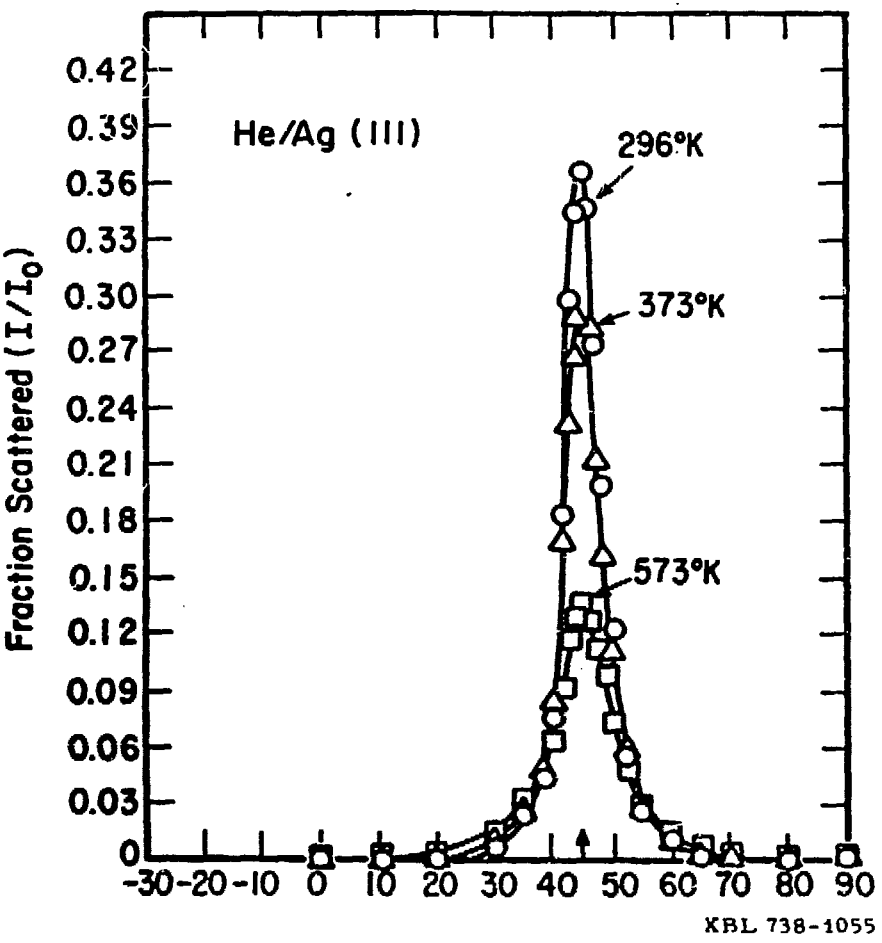
He/Ag (111)
296°K
373°K
573°K
Fraction Scattered (I/I0)
0.42
0.39
0.36
0.33
0.30
0.27
0.24
0.21
0.18
0.15
0.12
0.09
0.06
0.03
0
-30 -20 -10 0 10 20 30 40 50 60 70 80 90
XBL 738-1055

Fig. 9

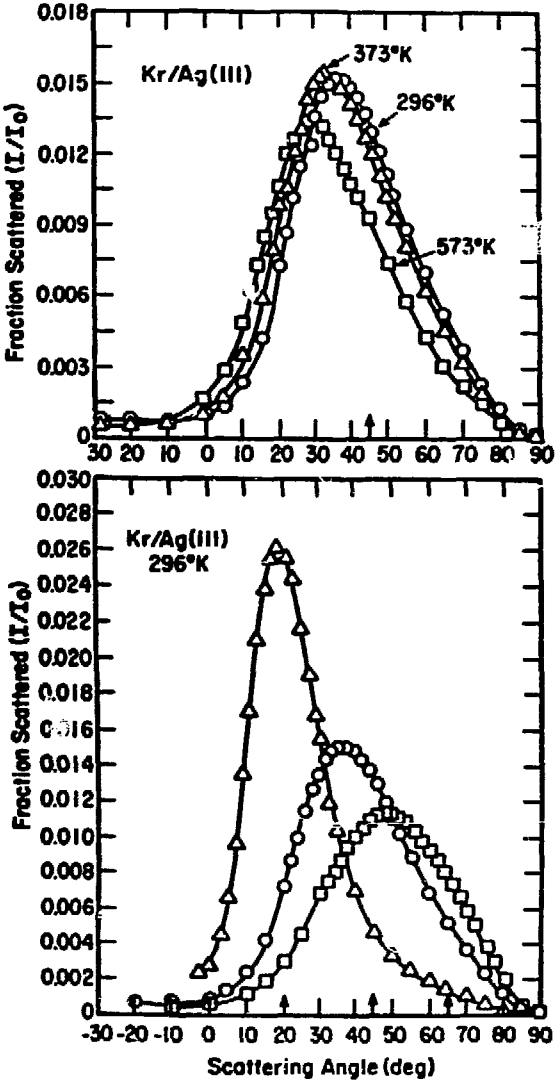

XBL 738-1054

Fig. 10

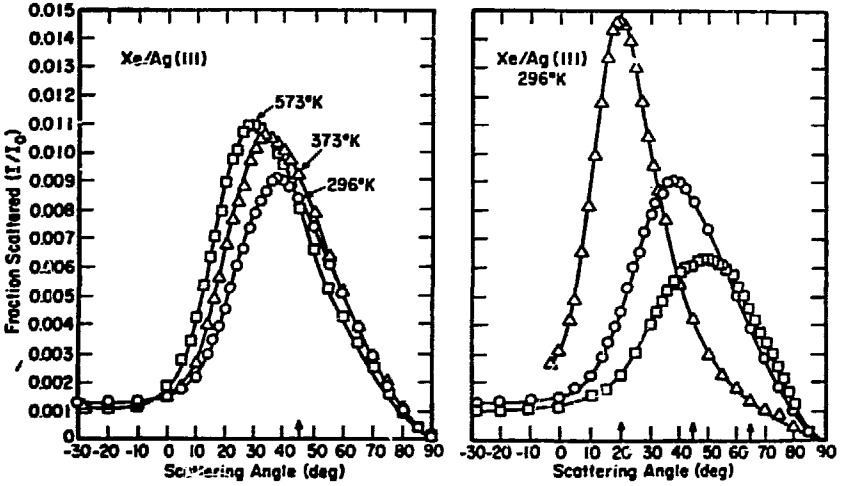

XBL 738-1057

Fig. 11

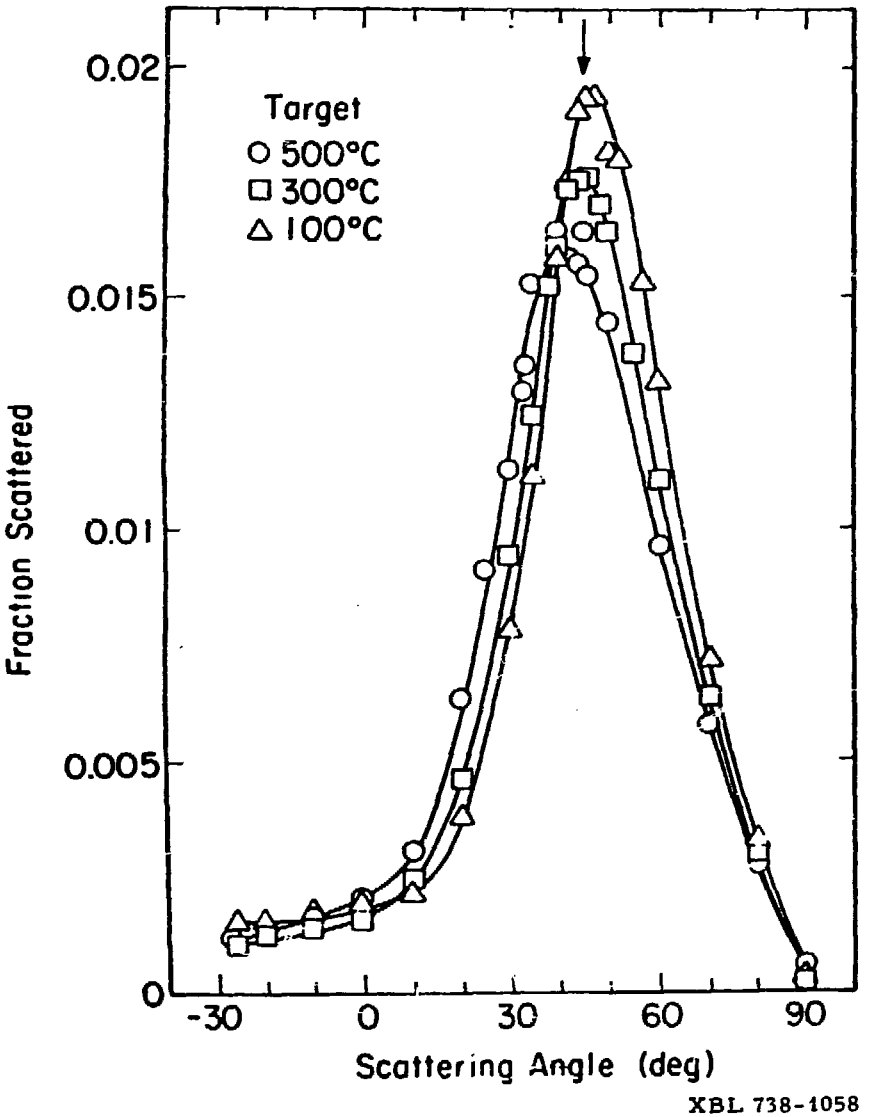

Fig. 12 Bottom

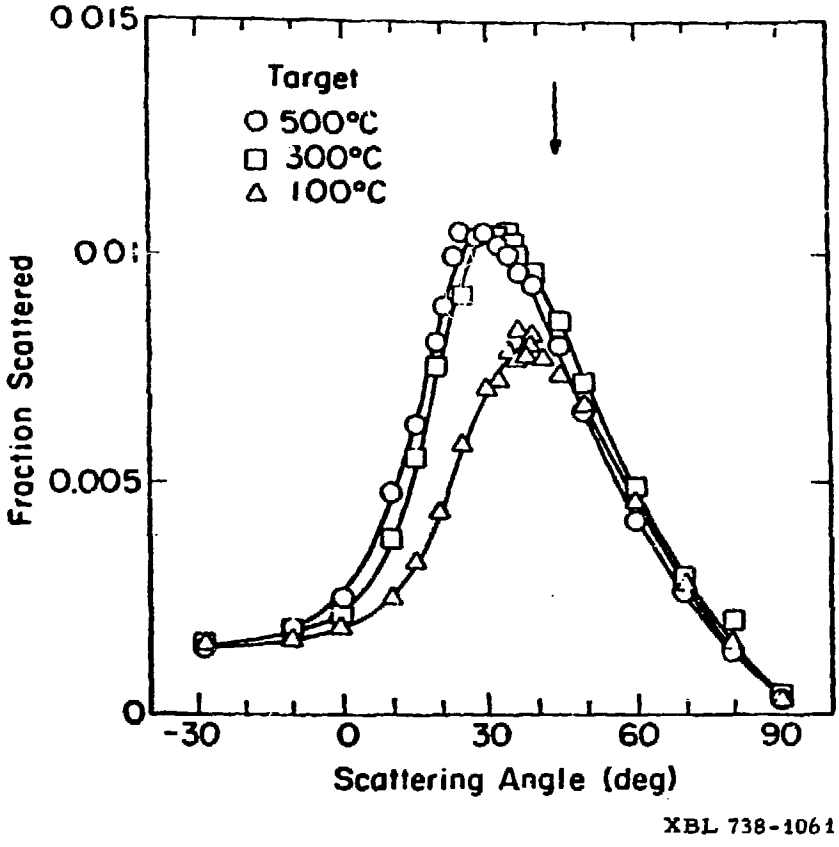
0.015
0.01
0.005
0
Fraction Scattered
Target
500°C
300°C
100°C
-30
0
30
60
90
Scattering Angle (deg)
XBL 738-1061

Fig. 12 Top

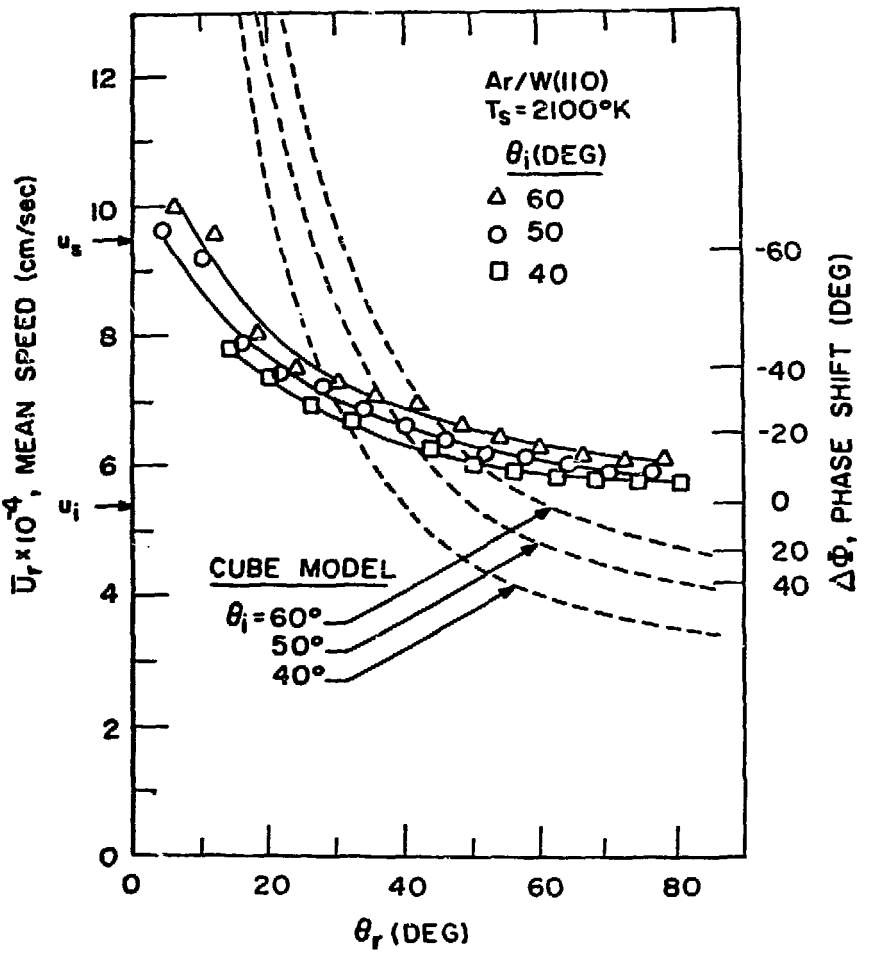

XBL 738-1064

Fig. 13

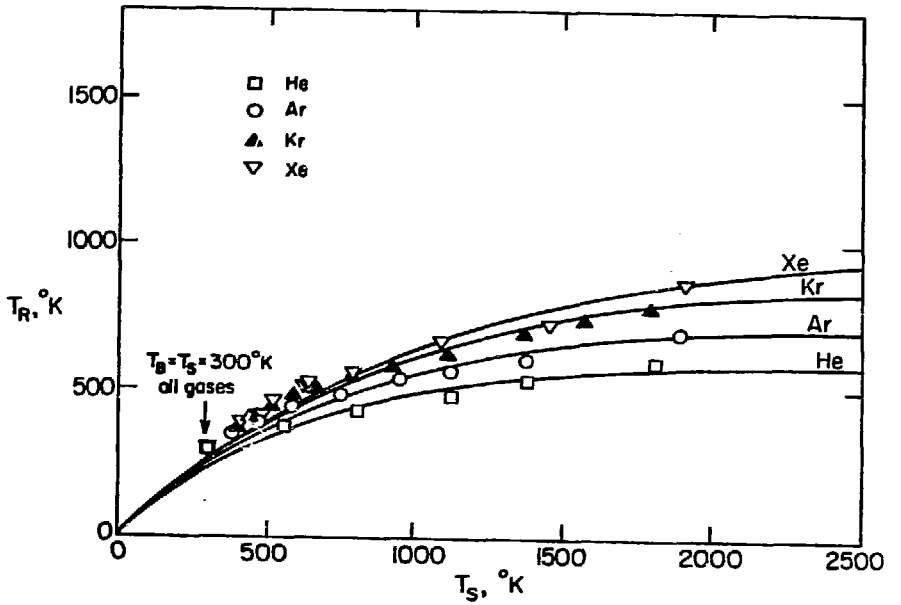

XBL 724-6184

Fig. 14

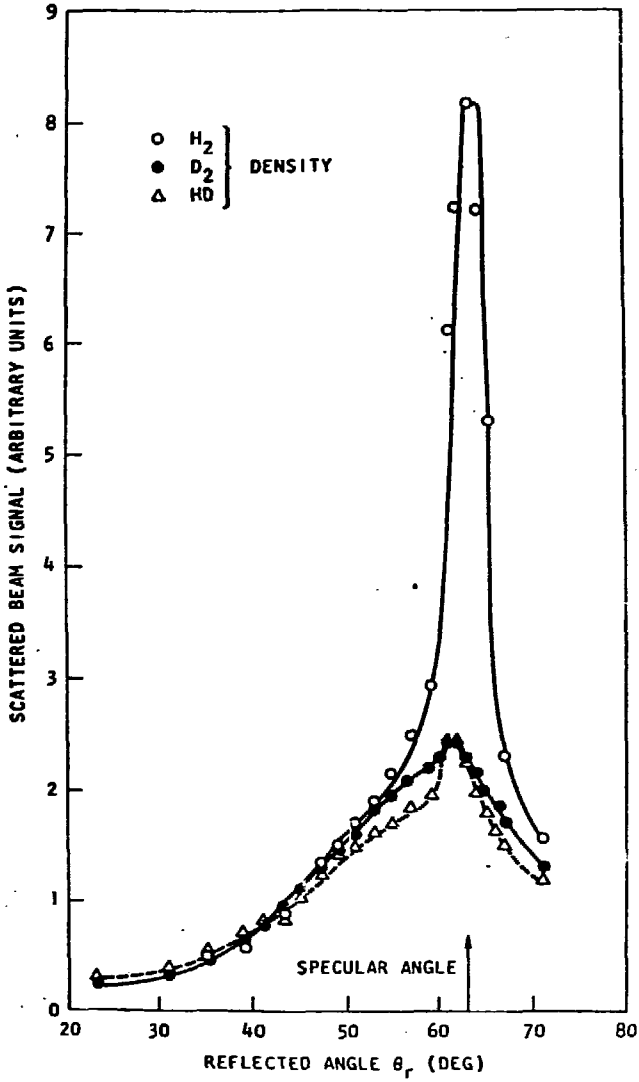
9
8
7
6
5
4
3
2
1
0
20
30
40
50
60
70
80
SCATTERED BEAM SIGNAL (ARBITRARY UNITS)
REFLECTED ANGLE θ_r (DEG)
H_2
D_2
HD
DENSITY
SPECULAR ANGLE
XBL 738-1063

Fig. 15

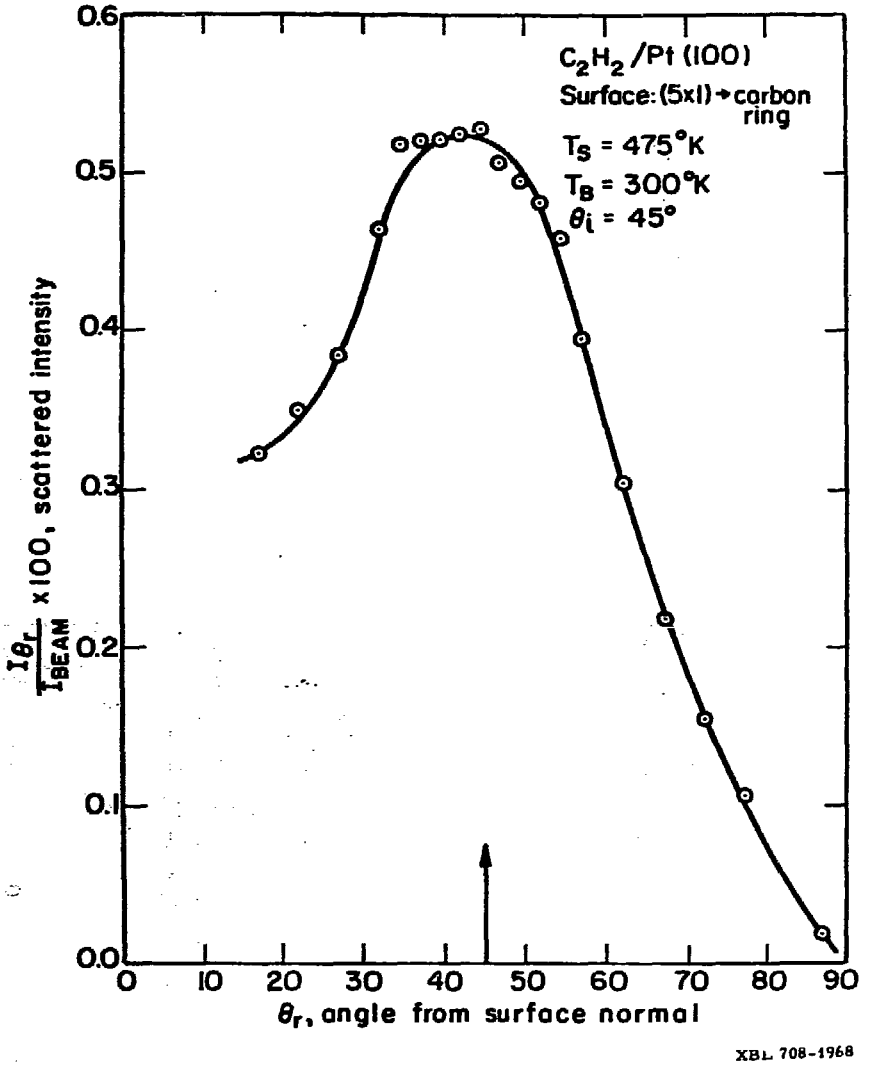
C_2H_2 /Pt (100)
Surface: (5x1) → carbon ring
T_S = 475°K
T_B = 300°K
θ_i = 45°
$\frac{I\theta_r}{I_{BEAM}}$ x100, scattered intensity
0.0
0.1
0.2
0.3
0.4
0.5
0.6
0
10
20
30
40
50
60
70
80
90
θ_r, angle from surface normal
XBL 708-1968

Fig. 16 Top

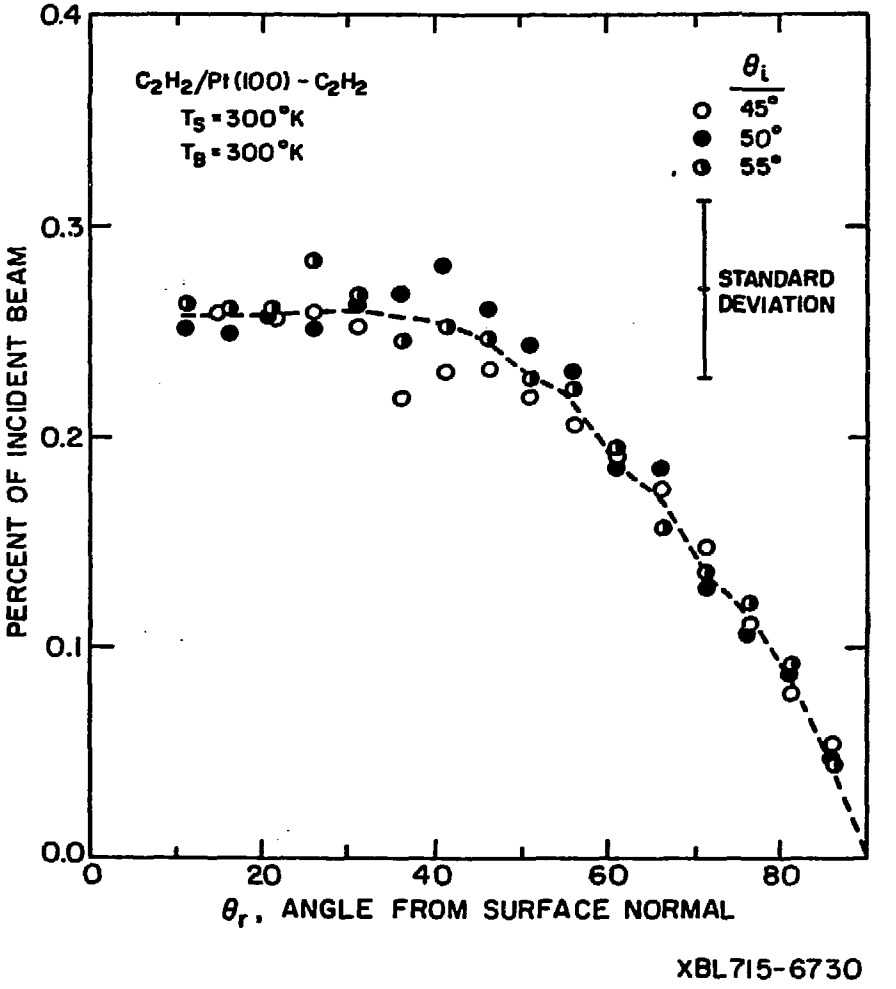

Fig. 16 Bottom

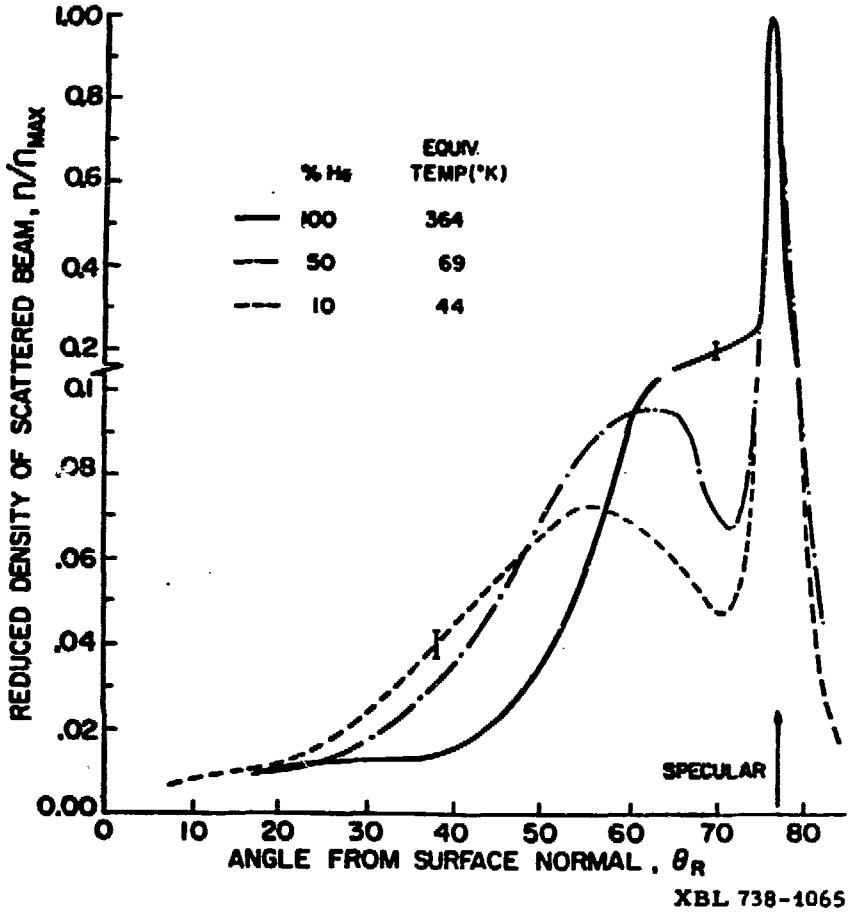
REDUCED DENSITY OF SCATTERED BEAM, n/n_MAX
1.00
0.8
0.6
0.4
0.2
0.1
.08
.06
.04
.02
0.00
% He
EQUIV. TEMP(°K)
100 364
50 69
10 44
SPECULAR
0 10 20 30 40 50 60 70 80
ANGLE FROM SURFACE NORMAL, θ_R
XBL 738-1065

Fig. 17

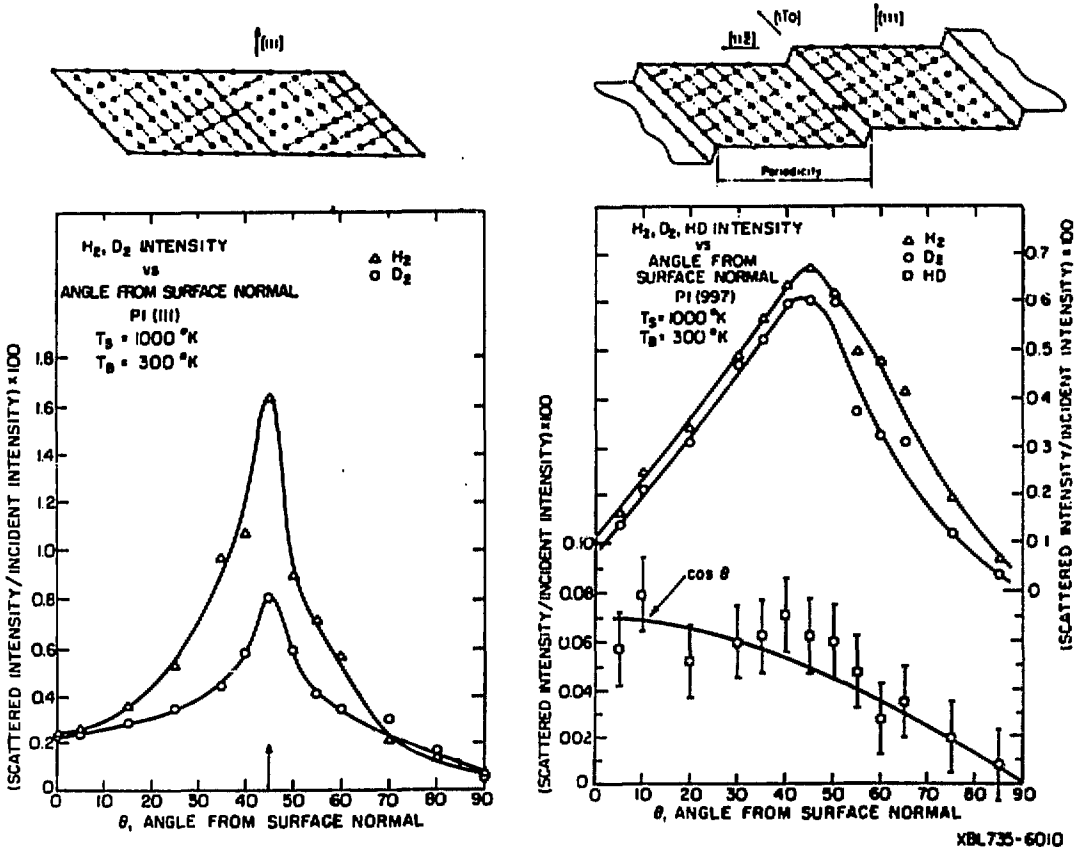
(111)
(110)
(111)
[112]
Periodicity
H2, D2 INTENSITY
vs
ANGLE FROM SURFACE NORMAL
Pt (111)
TS = 1000 °K
TB = 300 °K
H2
D2
(SCATTERED INTENSITY/INCIDENT INTENSITY) x 100
θ, ANGLE FROM SURFACE NORMAL
H2, D2, HD INTENSITY
vs
ANGLE FROM
SURFACE NORMAL
Pt (997)
TS = 1000 °K
TB = 300 °K
H2
D2
HD
cos θ
(SCATTERED INTENSITY/INCIDENT INTENSITY) x 100
θ, ANGLE FROM SURFACE NORMAL
XBL735-6010

Fig. 18